01 Mar 1998

Design of automotive structural components using high strength sheet steels effect of strain rate on material properties and the structural strength of cold-formed steel members

Wei-wen Yu

Missouri University of Science and Technology, wwy4@mst.edu

Civil Engineering Study 98-2
Cold-Formed Steel Series

Summary Report

DESIGN OF AUTOMOTIVE STRUCTURAL COMPONENTS USING HIGH STRENGTH SHEET STEELS

EFFECT OF STRAIN RATE ON MATERIAL PROPERTIES AND THE STRUCTURAL STRENGTH OF COLD-FORMED STEEL MEMBERS

by

Wei-Wen Yu
Project Director

A Research Project Sponsored by the
American Iron and Steel Institute

March 1998

Department of Civil Engineering
Center for Cold-Formed Steel Structures
University of Missouri-Rolla
Rolla, Missouri

PREFACE

The research work on automotive components conducted at the University of Missouri-Rolla under the sponsorship of the American Iron and Steel Institute began in 1982. During the first six years, studies were made on the basis of static loading. Since May 1988, studies have been concentrated on the effect of strain rate on material properties and the structural strength of cold-formed steel members along with the behavior of hybrid members. The research findings for the period from 1988 through 1997 are summarized in this report.

Special thanks are expressed to General Motors Corporation (Dr M. Y. Sheh, Mr. B. C. Schell, and Mr. P. H. Tran) for conducting the drop tower tests of stub columns in 1992.

The financial assistance granted by the Institute and the technical guidance provided by members of the AISI Task Force on Automotive Structural Design of the AISI Automotive Applications Committee and the AISI staff (Dr. S.J. Errera, Dr. A.L. Johnson, and Mr. D.C. Martin) are gratefully acknowledged. Members of the Task Force are: Messrs. E.C. Oren, Chairperson; G.A. Beecher; J. Borchelt; T.B. Kahlil; R.W. Lautensleger; H.F. Mahmood; D. Malen; M.Y. Sheh; and M.T. Vecchio. Former members of the Task Force included Messrs. F.L. Cheng; S.J. Errera; C. Haddad; C.W. Kim; K.H. Lin; J.N. Macadam; J.F. McDermott; J.G. Schroth; T.N. Seel; and R. Stevenson. An expression of thanks is also due to Mr. S.L. Caswell of National Steel Corporation and Mr. J.D. Grozier of LTV Steel Company for their help.

All materials used in the experimental study were donated by LTV Steel Company, Inland Steel Company, and National Steel Corporation.

Appreciation is also expressed to Drs. C. Santaputra, M.B. Parks, L.C. Pan, M. Kassar, C.L. Pan, and S. Wu for conducting this research project. Thanks are also due to Messrs. K. Haas, J. Bradshaw, F. Senter, S. Gabel, and J. McCracken, staff of the Department of Civil Engineering, for their technical support.

Special thanks are extended to Mrs. Cheryl Dennis, and Mrs. Laura Richardson, Secretaries of the Center for Cold-Formed Steel Structures, for their assistance in preparing this report.

TABLE OF CONTENTS

LIST OF TABLES

LIST OF FIGURES

I. INTRODUCTION

In recent years, various grades of sheet steels have been widely used by automotive manufacturers to produce more economic vehicles. The design information for using sheet steels is provided in the AISI Automotive Steel Design Manual (A2). In order to provide more design information on the structural use of high strength sheet steels, a research project was conducted at the University of Missouri-Rolla since 1982 under the sponsorship of the American Iron and Steel Institute. Results of the UMR research have been reflected in various versions of the AISI Design Manual (A2).

During the first six years of the study, the research work emphasized the study of mechanical properties of a selected group of high strength sheet steels along with the structural strength of cold-formed steel members subjected to static loading. The research findings were presented in ten progress reports (B1 - B10), three theses (C1 - C3), and eight journal and conference papers (D1 - D8). The primary reason for these investigations was due to the fact that the design provisions adopted from the AISI Specification (A1) were originally developed for building design using relatively low strength sheet steels. The study of automotive components was involved with the structural strength of flat and curved elements using high strength steels because the curved elements are also used for vehicles.

In view of the fact that automotive components are usually subject to dynamic loads, additional research work was carried out from 1988 though 1997 to study the effect of strain rate on material properties and the structural strength of cold-formed steel members including hybrid sections. The research findings on these subjects were presented in 12 progress reports (B11 - B22),

two theses (C4 & C5), and 10 journal and conference publications (D9 - D18).

In this report, the research results on the strain rate effects on material properties and member strength are summarized with cited references. Specifically, the effect of strain rate on material properties is presented in Section II. In Section III, discussions are dealing with the effect of strain rate on structural members including stub columns and beams. Finally the report is summarized in Section IV.

II. EFFECT OF STRAIN RATE ON MATERIAL PROPERTIES

A. General

During the period from 1988 through 1992, the effect of strain rate on mechanical properties was investigated for five grades of sheet steels. They were 35XF, 50XF, 100XF, 25AK, and 50SK. Among these five sheet steels, the effects of strain rate on the mechanical properties of 35XF, 50XF, and 100XF sheet steels were reported in the 11th and 12th Progress Reports (B11 and B12). A similar study of the mechanical properties of 25AK and 50SK sheet steels was presented in the 17th Progress Report (B17). The aging effect on the material properties of these two sheet steels (25AK and 50SK) was discussed in the 21st Progress Report (B21).

Details of the research findings for the effect of strain rate on material properties are summarized in subsequent subsections.

B. Tensile Properties (B11, B14, B17, and B18)

a. XF Sheet Steels (B11, B14, and B18)

The effect of strain rate on the tensile properties of 35XF, 50XF, and 100XF sheet steels was studied from May 1988 through December 1988. The research work included a review of literature and testing of 124 tensile specimens. Detailed information on the experimental investigation of XF sheet steels was presented in the 11th Progress Report (B11). In these tensile coupon tests, mechanical properties were determined for longitudinal (parallel to the direction of the rolling) and

transverse (perpendicular to the direction of the rolling) directions under three different strain rates of 10^{-4}, 10^{-2}, and 1.0 in./in./sec. Figures 2.1, 2.2, and 2.3 show graphically the effect of strain rate on the stress-strain curves of 35XF, 50XF, and 100XF sheet steels tested in longitudinal tension. The increases in longitudinal tensile yield stress for these three XF sheet steels are summarized in Table 2.1. These tested yield stresses are used in Section III of this report for the evaluation of member strength of stub columns and beams. In addition to the virgin material properties, two of the three materials (35XF and 50XF) were also tested in tension to determine the combined effects of cold-stretching and strain rate. In order to determine the combined effects of strain rate and aging, half of the coupons were tested during a period of two days after cold-stretching operation. The remaining half of the cold-stretched coupons were tested to failure at least 30 days after cold-stretching operation. No significant increase in static yield stress was observed due to the strain aging effect. However, the results indicated that all mechanical properties (F_y, F_u, and elongation) were affected by the strain rate and the amount of cold-stretching when the strain rate increased from 10^{-4} to 1.0 in./in./sec. For the details, see References B11, B14, and B18.

b. AK and SK Sheet Steels (B17 and B18)

Up to November 1991, the UMR studies were limited only to the structural members which were fabricated and assembled with the same material in a given test specimen. At its November 13, 1991 meeting, the AISI Task Force on Automotive

Structural Design decided to investigate hybrid sections which are fabricated and assembled from two different sheet steels, one with a 25 ksi yield stress, and the other with a 50 ksi yield stress. Consequently, a total of 48 tensile coupons of 25AK and 50SK sheet steels were tested in early 1992 to study the effect of strain rate on mechanical properties of these two sheet steels which have nominal yield stresses of 25 ksi and 50 ksi. In those tests, the strain rate also ranged from 10^{-4} to 1.0 in./in./sec. The stress-strain curves for 25AK and 50SK sheet steels are shown in Figures 2.4 and 2.5, respectively. The tested yield stresses for these two types of sheet steels are also given in Table 2.1 and used in Section III to evaluate the structural strength of hybrid sections.

C. **Compressive Properties** (B12, B14, B17, and B18)

a. XF Sheet Steels (B12, B14, and B18)

During the period from January 1989 through July 1989, the UMR research work dealt with a study of compressive mechanical properties of 35XF, 50XF, and 100XF sheet steels. The results of 54 tests were presented in the 12th Progress Report (B12). Figures 2.6, 2.7, and 2.8 illustrate the effect of strain rate on the stress-strain curves of 35XF, 50XF, and 100XF sheet steels tested in longitudinal compression. The tested compressive yield stresses and proportional limits are summarized in Table 2.2.

b. AK and SK Sheet Steels (B17 and B18)

In early 1992, a total of 24 compression coupons of 25AK and 50SK sheet

steels were tested and reported in Reference B17. Compressive stress-strain curves are shown in Figures 2.9 and 2.10 for 25SK and 50Sk sheet steels, respectively. The compression coupons were tested under four different strain rates ranging from 10^{-4} to 1.0 in./in./sec. The tested compressive yield stresses and proportional limits are also given in Table 2.2.

D. **Predicted Tensile and Compressive Yield Stresses** (B11, B12, B17, and B18)

a. Strain Rate Sensitivity

The strain rate sensitivity was reviewed and discussed in the 11th, 12th, and 17th Progress Reports. Based on the test results on tensile and compressive mechanical properties of five different sheet steels, the strain rate sensitivity exponents m were computed as follows:

$$m = \ln(\sigma_2/\sigma_1)/\ln(\dot{\varepsilon}_2/\dot{\varepsilon}_1) \qquad (2.1)$$

In the above equation, σ_1 and σ_2 are the stresses corresponding to strain rates $\dot{\varepsilon}_1$ and $\dot{\varepsilon}_2$, respectively. It was found that in general, the strain rate sensitivity increases as the strain rate increases and that it decreases progressively as the static yield stress level increases. The computed strain rate sensitivity exponents were presented in tables and figures, which were included in the progress reports.

b. Prediction of the Dynamic Yield Stress

In order to predict the dynamic tensile and compressive stresses for a given strain rate, the following second degree polynomial equation was developed in the 12th Progress Report for 35XF, 50XF, and 100XF sheet steels by using the least

square method in the strain rate range of 0.0001 to 1.0 in./in./sec.

$$Y = A + BX + CX^2 \tag{2.2}$$

where Y = yield stress

$X = \log \dot{\varepsilon}$

$\dot{\varepsilon}$ = strain rate

A, B, and C = constants

The polynomial parameters A, B, and C were determined from the test data of 35XF, 50XF, and 100XF sheet steels. These constants were given in the 12th Progress Report for each individual case tested under compression and tension. For 25AK and 50SK sheet steels, the polynomial parameters were given in the 17th Progress Report. The polynomial equations for these five sheet steels tested under longitudinal tension and longitudinal compression are shown in Figures 2.11 through 2.20.

In order to simplify the design procedure, it is desirable to have a general equation to predict the yield stresses for different sheet steels under various strain rates. In the 18th Progress Report (B18), a combination of material properties obtained from five different sheet steels (25AK, 35XF, 50XF, 50SK, and 100XF) were used to develop the following general equation (Eq. 2.3). Allowing some extrapolation of the test data, this equation is proposed for strain rates ranging from 10^{-4} to 10^{2} in./in./sec.

$$(F_y)_{pred} = (A\, e^{(B/F_y)} + 1)(F_y) \tag{2.3}$$

where F_y = static yield stress

$$A = a_1 + b_1 \log(\dot{\varepsilon}) + c_1 \log(\dot{\varepsilon})^2 \quad (2.4)$$

$$B = a_2 + b_2 \log(\dot{\varepsilon}) + c_2 \log(\dot{\varepsilon})^2 \quad (2.5)$$

e = base of natural logarithm = 2.718

$\dot{\varepsilon}$ = strain rate

For tensile yield stress:

$a_{1t} = 0.023$ $a_{2t} = 77.7$

$b_{1t} = 0.009$ $b_{2t} = 0.069$

$c_{1t} = 0.001$ $c_{2t} = -0.595$

For compressive yield stress:

$a_{1c} = 0.033$ $a_{2c} = 64.9$

$b_{1c} = 0.004$ $b_{2c} = 11.1$

$c_{1c} = 0.000$ $c_{2c} = -1.87$

Based on Equations 2.3, 2.4, and 2.5, Figures 2.21 and 2.22 show graphically the predicted yield stresses for tension and compression, respectively, using different strain rates. Good agreements between the tested and predicted yield stresses were obtained in the 18th Progress Report by using these general equations. For design purpose, Equations 2.3, 2.4, and 2.5 are presently included in Revision 5 of the AISI Automotive Steel Design Manual (A2).

E. **Aging Effect** (B11and B21)

In Section II.B.a, it was mentioned that the combined effect of strain rate and aging

was studied briefly for 35XF and 50XF sheet steels in the 11th Progress Report (B11) by applying cold-stretching in tensile coupons, which were tested at different times. At the suggestion of the AISI Task Force, the aging effect on the mechanical properties of 25AK and 50SK sheet steels were studied in August 1995 and January 1997. The mechanical properties obtained from the coupon tests conducted in 1992, 1995, and 1997 were compared in the 21st Progress Report (B21) as shown in Figures 2.23 and 2.24. It was found that at the strain rate of 0.0001 in./in./sec, the yield stresses and tensile strengths of 25AK and 50SK sheet steels increased by 4 to 6% over a time period of four years and ten months due to the aging effect. At the strain rate of 0.01 in./in./sec, the yield stresses and tensile strengths of the same sheet steels increased by 4 to 10% over the same period of time. Based on the coupon tests conducted in 1995, at the strain rate of 0.0001 in./in./sec., the yield stress of 25AK and 50SK sheet steels increased by 6 to 9% over a time period of three years and five months. For details, see Table 2.3.

It was also found that the percentage increases in the yield strength of the 25AK and 50SK steels are approximately the same as the percentage increases in the tensile strength of both steels. The increases in both yield and tensile strengths of the 25AK steel appear to be slightly higher than that for the 50SK steel over the same period of time.

F. Summary on the Effect of Strain Rate on Material Properties

Based on the test results reported in References B11, B12, B17, B18, and B21, the following conclusions have been drawn for the effect of strain rate on the mechanical

properties of five selected sheet steels.

1. The mechanical properties (proportional limit, yield stress, and ultimate tensile strength) increase with increasing strain rates.
2. For most cases, the mechanical properties in transverse direction are slightly higher than those in the longitudinal direction under the same strain rate.
3. Yield stress is more sensitive to strain rate than ultimate tensile strength.
4. In general, the strain rate sensitivity values for yield stress in tension are similar to the values in compression.
5. The strain rate sensitivity value is not a constant for each sheet steel. In most cases, the strain rate sensitivity value increases with increasing strain rate.
6. The mechanical properties of the sheet steels having lower yield stresses are more sensitive to strain-rate than the sheet steels having higher yield stresses. Table 2.4 lists the percentage increase in yield stress when the strain rate increases from 0.0001 to 1.0 in./in./sec.
7. Polynomial equations have been developed for the dynamic tensile and compressive yield stresses of five selected sheet steels. These equations can predict the dynamic yield stress at higher strain rates than that used in the tests.
8. For design purposes, a general equation (Equation 2.3) was developed to predict tensile and compressive yield stresses for the strain rates from 10^{-4} to 10^{2} in./in./sec.
9. Based on the preliminary study of 35XF and 50XF sheet steels, no significant increase in yield stress was observed due to strain aging over a time period of 30

days. However, material properties were found to be affected by the strain rate and the amount of cold stretching.

10. A study of 25AK and 50SK sheet steels indicated that at the strain rate of 0.0001 in./in./sec., the yield stress increased by 4 to 6% over a time period of four years and ten months due to the aging effect. At the strain rate of 0.01 in./in./sec., the yield stress increased by 4 to 10% over the same period of time. Based on the coupon tests conducted in 1995, at the strain rate of 0.0001 in./in./sec., the yield stresses of 25AK and 50SK sheet steels increased by 6 to 9% over a time period of three years and five months. No coupon tests were conducted in 1995 for the strain rate of 0.01 in./in./sec.

III. EFFECT OF STRAIN RATE ON COLD-FORMED STEEL MEMBERS

A. General

The structural behavior and strength of cold-formed steel members subjected to higher strain rates were studied since August 1989. Two materials (35XF and 50XF) were used in the first phase of investigation. The main purpose of this study was to determine whether the AISI design formulas which were originally developed from static tests, can also be used for structural members subjected to dynamic loads.

Up to April 1990, 37 stub columns and 30 beam specimens fabricated from 35XF sheet steel were tested by Kassar under different strain rates. Hat- and box- sections were used to determine the strength of structural members having stiffened compression elements. Channels and I- sections were used to study the strength of members having unstiffened compression elements. Test results and evaluations were presented in the 13th and 14th Progress Reports (B13 and B14).

During the period from May 1990 through October 1990, 12 stub columns using 35XF steel and 48 stub columns using 50XF steel were tested by Pan. Test results and evaluations were presented in the 15th and 18th Progress Reports (B15 and B18).

In addition to the study of the stub columns using 50XF sheet steel, the study of the beam specimens fabricated from 50XF sheet steel subjected to dynamic loads was initiated in March 1991. Fifteen (15) channel specimens and 15 hat-sections were tested as beams under the strain rates from 10^{-5} to 10^{-2} in./in./sec. The test results were evaluated and presented in the 16th and 18th Progress Reports (B16 and B18).

Prior to 1992, the study was limited only to the structural members which were assembled with the same material in a given section. In order to determine the structural strength and behavior of hybrid sections using different sheet steels, 52 drop tower tests of stub columns using 25AK and 50SK sheet steels were conducted at General Motors Corporation during the summer of 1992. The impact velocities used for the tests were 28.5 and 43.2 km/hr. The research findings were presented by Schell and Pan at the 1993 and 1994 International Body Engineering Conferences, respectively (D17 and D13).

At the University of Missouri-Rolla, the study of hybrid stub columns fabricated from 25AK and 50SK sheet steels was initiated in January 1993. A total of 96 box-shaped stub columns and 48 hat-shaped stub columns were tested under strain rates from 10^{-4} to 10^{-1} in./in./sec. Among these tests, 80 specimens were hybrid sections. The test results were evaluated and presented in the 19th Progress Report (B19).

With regard to hybrid beams, the testing of hat-shaped specimens was initiated in October 1993. A total of 72 beams fabricated from 25AK and 50SK sheet steels were tested for dynamic loads under strain rates from 10^{-4} to 10^{-2} in./in./sec. The test results were presented in the 20th Progress Report (B20).

Research findings on the effect of strain rate on cold-formed steel members are summarized in subsequent sections.

B. UMR Study - Homogeneous Members

As stated in Section III.A, hat-sections, box-sections, channels, and I- sections have been used to study the strength of cold-formed steel members for the purpose of verifying

the adequacy of the AISI design provisions for automotive components which are subjected to dynamic loads. Following a detailed review of literature and the conduct of extensive experimental investigations, the research results with evaluations were presented in seven progress reports (B13 - B16 , B18 - B20).

a. 13th Progress Report (B13) - Stub Columns and Homogeneous Beams Fabricated from 35XF Steel

The 13th Progress Report contains a literature review of the structural behavior and strength of compression elements under static and dynamic loads. It also includes the background information on the AISI design provisions.

The experimental investigation and the evaluation of the experimental data presented in this report dealt with 37 stub columns and 30 beams fabricated from 35XF sheet steel. The ranges of w/t ratios varied from 8.93 to 20.87 for unstiffened compression elements and from 26.92 to 76.64 for stiffened compression elements with strain rates ranged from 10^{-5} to 0.1 in./in./sec.

Experimental Investigation

1. Stub Columns

Eighteen (18) box-sections and 19 I-sections (Figure 3.1 (a)) were tested as stub columns under different strain rates. Test results were compared with the critical local buckling load (Eq. 3.1) and the ultimate axial load (Eq. 3.2) calculated as follows:

$$P_{cr} = A_t f_{cr} \tag{3.1}$$

$$P_u = A_e F_y \tag{3.2}$$

where A_e = effective cross-sectional area of the stub column

A_t = full cross-sectional area of the stub column

f_{cr} = critical local buckling stress of compression element

F_y = static or dynamic yield stress of steel

2. Beams

Fifteen (15) hat-sections and 15 channel-sections (Figure 3.1 (b)) were tested as simply supported beams under different strain rates. Test results were compared with the critical local buckling moment (Eq. 3.3) and the bending moment strength (Eq. 3.4 or 3.6) calculated as follows:

$$M_{cr} = S_{xc} f_{cr} \tag{3.3}$$

where S_{xc} = elastic section modulus of the full cross section relative to the compression flange

f_{cr} = critical buckling stress of the compression flange

For the bending moment strength, two approaches were used in the evaluation of experimental results. i.e., initiation of yielding and inelastic reserve capacity. For these two approaches, the "Initiation of Yielding" approach can be used to determine the yield moment for any cross section. However, the "Inelastic Reserve Capacity" approach for computing the ultimate moment can only be used for certain sections subjected to some specific limitations.

(i) Based on the Initiation of Yielding

The yield moment is

$$M_y = F_y S_e \tag{3.4}$$

where F_y = static or dynamic yield stress of steel

S_e = elastic section modulus of the effective section

(ii) Based on the Inelastic Reserve Capacity

For neutral axis: $\int \sigma dA = 0$ (3.5)

For ultimate moment: $M_u = \int \sigma y dA$ (3.6)

In Equations 3.5 and 3.6, σ is the stress in the element, A is the area of the element, and y is the distance from the centroid of the element to the neutral axis.

Figure 3.2 shows the stress distribution in sections with yielded tension and compression flanges at ultimate moment. The following equations can be used to compute the values y_c, y_t, y_p, y_{cp}, and y_{tp} as shown in Figure 3.2 and the ultimate moment, M_u. For the purpose of simplicity, midline dimensions were used in the calculations.

$$y_c = (b_t - b_c + 2d)/4 \tag{3.7}$$

$$y_t = d - y_c \tag{3.8}$$

$$y_p = y_c/C_y \tag{3.9}$$

$$y_{cp} = y_c - y_p \tag{3.10}$$

$$y_{tp} = y_t - y_p \tag{3.11}$$

$$M_u = F_y t\left[b_c y_c + 2y_{cp}(y_p + y_{cp}/2) + (4/3)(y_p)^2 + 2y_{tp}(y_p + y_{tp}/2) + b_t y_t\right] \tag{3.12}$$

where b_c = effective width of the compression flange

b_t = total width of the tension flange

d = depth of the section

t = thickness of the section

C_y = compression strain factor for stiffened compression elements without intermediate stiffeners, which can be determined as follows:

$$C_y = 3 \qquad \text{for } w/t \le \lambda_1 \tag{3.13}$$

$$C_y = 3 - 2(w/t - \lambda_1) / (\lambda_2 - \lambda_1) \qquad \text{for } \lambda_1 < w/t < \lambda_2 \tag{3.14}$$

$$C_y = 1 \qquad \text{For } w/t \ge \lambda_2 \tag{3.15}$$

where $\lambda_1 = 1.11/ (F_y/E)^{1/2}$ (3.16)

$\lambda_2 = 1.28/(F_y/E)^{1/2}$ (3.17)

According to the AISI Specification (A1) and the Automotive Steel Design Manual (A2), the ultimate moment computed by using the inelastic reserve capacity procedure should not exceed the limit of $(1.25\ S_e F_y)$.

In addition, the "Inelastic Reserve Capacity" approach can be used only when the following conditions are met:

(1) The member is not subject to twisting or to lateral, torsional, or torsional-flexural buckling.

(2) The effect of cold forming is not included in determining the yield point.

(3) The ratio of the depth of the compressed portion of the web to its thickness does not exceed $1.11/(F_y/E)^{1/3}$

(4) The shear force does not exceed $0.35F_y$ times the web area, ht.

(5) The angle between any web and the vertical does not exceed 30 degrees.

In addition to the study of moment capacity, deflections of beams were measured and compared with the calculated values.

Summary

Based on the test data and the evaluation in accordance with the Automotive Steel Design Manual (A2), the following conclusions were drawn for the effect of dynamic loads on the structural strength of cold-formed steel stub columns and beams fabricated from 35XF sheet steel:

1. For most of the tests, the critical local buckling strength, yield strength, and ultimate strength increased with increasing strain rates. The ultimate strengths showed larger increases at higher strain rates than at lower strain rates for specimens with various w/t ratios.
2. The effect of strain rate on member strength was found to be slightly higher than that for material properties. It is expected that the increase of member strength may be partially due to aging effect.
3. The computed ultimate strength in accordance with the Automotive Steel Design Manual was found to be conservative for all stub column and beam tests. The

prediction of the ultimate capacity was improved by using the dynamic yield stress.

4. Except for two channel beams, the computed midspan deflections of beams are slightly larger than those measured from tests.

b. 14th Progress Report (B14) - First Summary on the Study of the Effect of Strain Rate on Material Properties and Structural Strength of Stub Columns and Beams Using 35XF Sheet Steel

This report was based on Kassar's Ph.D. thesis completed in May 1990 (C4). It included (1) a comprehensive review of literature on materials and members, (2) experimental programs on material properties of three sheet steels (35XF, 50XF, and 100XF) in tension and compression, (3) results of 30 beam tests and 37 stub column tests using 35XF sheet steel for stiffened and unstiffened compression elements, (4) evaluation of material test data, (5) evaluation of the experimental data for structural members, and (6) conclusions.

This document is the first summary on the study of the effect of strain rate on material properties and structural strength of cold-formed steel members which was conducted by Kassar at UMR since May 1988. The primary goal of this study was to determine the adequacy of the AISI effective width formulas for the design of automotive components subjected to dynamic loads.

As the first phase of the research work, dynamic material properties of three sheet steels (35XF, 50XF, and 100XF) were determined experimentally by using the MTS 880 Test System. The strain rate used for the tests ranged from 10^{-4} to 1.0 in./in./sec. At the same

time, a large number of related publications and research reports were reviewed in detail.

For the experimental program, comprehensive discussions were presented for material properties concerning test equipment and test procedure with a complete set of figures and tables for three sheet steels tested in tension and compression both in longitudinal and transverse directions. The steel sheets used for the tests included virgin materials, 2% cold-stretched and 8% cold-stretched coupons tested under different strain rates at various times. The test data on stub columns and beams using 35XF sheet steel were based on the 13th Progress Report.

All test results on material properties, stub columns, and beams were evaluated and compared with the computed values in accordance with the Automotive Steel Design Manual. Conclusions were drawn for the effect of strain rate on material properties and the effect of dynamic load on member strength. The following conclusions were based on the research findings on three different sheet steels combined with 67 cold-formed steel members using 35XF sheet steel:

Materials

1. Proportional limit, yield strength, and ultimate strength increase with increasing strain rate.
2. Yield strength is more sensitive to strain rate than ultimate strength.
3. The strain rate sensitivity value is not a constant. In most cases it increases with increasing strain rate.
4. The mechanical properties of sheet steels having low yield strengths are more

sensitive to strain-rate effects.

5. A second degree polynomial is well fitted to the experimental data for both tension and compression and can be used to predict the yield and ultimate strength at high strain rates above the range of the strain rate used in the tests.

Structural Members

1. The critical local buckling strength, yield strength, and ultimate strength for most of the tests increased with increasing strain rates. The ultimate strengths showed larger increases at higher strain rates than at lower strain rates.
2. The effect of strain rate on member strength was found to be similar to those observed from the previous study of material properties as affected by different strain rates. However, ratios of dynamic to static ultimate strength for beams and stub columns conducted in this study were found to be slightly higher than those for tensile or compressive material yield stresses.
3. The computed ultimate strength based on the Automotive Steel Design Manual, using static or dynamic yield stress, was found to be conservative for all beam and stub column tests. The mean and standard deviation values for the ratios of tested-to-computed ultimate strengths were improved by using the dynamic yield stresses rather than the static values for all cases studied in this investigation.
4. The computed midspan deflection under service moments are slightly larger than those measured from tests, except for two channel beams.

c. 15th Progress Report (B15) - Additional Study of Stub Columns Having Large w/t

Ratios and Fabricated from 35XF and 50XF Sheet Steels

In the 13th Progress Report, the w/t ratios used for stub columns with unstiffened and stiffened elements were limited to 20.87 and 76.64, respectively. In order to study the behavior of steel members with relatively large w/t ratios, six I-shaped sections having unstiffened elements with w/t ratios of about 44 and six box-shaped sections having stiffened elements with w/t ratios of about 100 (Figure 3.1 (a)) were fabricated from 35XF steel and tested as stub columns in August 1990. In addition, 22 box-sections having stiffened elements with w/t ratios up to 98 and 26 I-sections having unstiffened elements with w/t ratios up to 35 were fabricated from 50XF sheet steel and tested as stub columns during the period from August through October 1990.

In the evaluation of the test data, Equations 3.1 and 3.2 were used to compute the predicted critical local buckling load and the ultimate axial load using static and dynamic yield stresses. Based on the research findings on the additional stub column tests for relatively large w/t ratios and the use of two types of sheet steels, it was found that the predicted ultimate axial loads for the stub columns fabricated from 50XF sheet steel are less conservative than the stub columns fabricated from 35XF sheet steel. It was also noted that the predicted ultimate loads of the stub columns for studying stiffened elements are less conservative than the stub columns for studying unstiffened elements. Tables 3.1 and 3.2 present a summary of the mean values and standard deviations of $(P_u)_{test}/P_u)_{comp}$ ratios based on the stub column tests for the study of stiffened elements in Table 3.1 and the study of unstiffened elements in Table 3.2.

In this report, an attempt was made to study the effect of cold-work on the axial

capacity of stub columns. From the results presented in Appendix A of the 15th Progress Report, it was observed that for the box-shaped and I-shaped stub columns with relatively small w/t ratios, a better prediction of ultimate axial loads can be obtained by considering the cold-work effect.

d. 16th Progress Report (B16) - Additional Study of Beams Using 50XF Sheet Steel

In 1990, Kassar tested and studied 30 beam specimens using just 35XF sheet steel. During the period from February through May 1991, 15 additional hat-shaped beams and 15 channel beams (Figure 3.1(b)) were fabricated from 50XF sheet steel and tested by C.L. Pan. The w/t ratios of the stiffened compression flanges ranged from 26.28 to 66.08. For the unstiffened compression elements, the w/t ratios varied from 8.78 to 20.57. The strain rates were in the range of 10^{-5} to 10^{-2} in./in./sec.

In the evaluation of the test data, Equations 3.3 and 3.4 were applied for the calculation of the critical local buckling moment and the yield moment, respectively. In addition, due consideration was given to the effect of cold-work of forming for the channel-beams having unstiffened compression flanges with small w/t ratios. For some hat-shaped beams, the inelastic reserve capacity was calculated for the purpose of comparison if such a member can satisfy the specific AISI requirements.

Based on the evaluation of the beam tests using 35XF and 50XF sheet steels, conclusions were drawn for the effect of strain rate on the strength of cold-formed steel beams using these two types of sheet steels:

1. For beam specimens using hat-sections and channels with small w/t ratios,

a better prediction of yield moments can be achieved from the consideration of the cold work of forming with an exception for the hat-shaped beams fabricated from 50XF sheet steel. Tables 3.3 and 3.4 show the improvements of prediction by considering cold-work of forming for hat-sections and channels with small w/t ratios. For Table 3.3, the w/t ratio of the stiffened flange varied from 29.05 to 30.17 for hat sections. For Table 3.4, the w/t ratio of the unstiffended flange varied from 9.03 to 9.28 for channels.

2. From the beam tests using hat-sections and channels, the computed moments for the beams fabricated from 50XF sheet steel were found to be less conservative than the beams fabricated from 35XF sheet steel as indicated in Tables 3.5 and 3.6.
3. The computed ultimate moments of beam specimens having stiffened flanges are slightly less conservative than the beam specimens with unstiffened flanges. Other conclusions which were drawn in the 13th and 14th Progress Reports for the beams fabricated from 35XF sheet steel are applicable to those beams fabricated from 50XF sheet steel.

e. 18th Progress Report (B18) - Second Summary on the Study of the Effect of Strain Rate on Material Properties and Structural Strength of Stub Columns and Beams Using 35XF and 50XF Sheet Steels

This report was based on C.L. Pan's Ph.D. thesis completed in December 1992 (C5). It covered the study of the effect of strain rate on the material properties of five types of sheet

steels with nominal yield strengths ranging from 25 ksi to 100 ksi. Test results of 97 stub columns and 60 beams fabricated from 35XF and 50XF sheet steels were evaluated for the purpose of studying the member strength affected by the strain rate.

In this report, in addition to the coverage of general subjects such as introduction, review of literature, experimental program, evaluation of experimental data, and conclusions, further discussions were included for material properties and test results of stub columns and beams.

Specifically, this report is the second summary on the study of the effect of strain rate on material properties and member strength. The information used for the analysis and comparison with the AISI design provisions covered all the tests of five sheet steels and 157 members conducted by Kassar and Pan during the period from 1988 through 1992. In the evaluation of material test results, a general equation (Eq. 2.2) was developed in the report for predicting the dynamic yield stresses. For the structural strength of stub columns and beams, both static and dynamic yield stresses were applied for the determination of the axial capacity of stub columns and the bending strength of beams. The cold-work of forming and the inelastic reserve capacity of beams were considered when the specific requirements are met. Other topics discussed in the report were related to the member strength as affected by the stress-strain relationship of the sheet steel and the improvement of the predicted member strength by using appropriate local buckling coefficients for unstiffened compression elements.

Based on the available information and a detailed study, it was reconfirmed that the mechanical properties of sheet steels and the ultimate strength of cold-formed steel structural

members increase with increasing strain rates. For compact sections fabricated from 35XF sheet steel, the effect of cold-work should be considered in the calculation of the ultimate loads of stub columns and the yield moments of beams, provided that the AISI specific requirements are met. For noncompact stub columns and beams, the values of local buckling coefficient obtained from Kalyanaraman's equations (Equations A1 through A7 in Appendix A) can be used for calculating the effective width of unstiffened compression elements. Based on these buckling coefficients, good comparisons were obtained between the tested and predicted ultimate loads for stub columns frabricated from 35XF and 50XF sheet steels.

A better prediction for the ultimate capacity of stub columns and beams can be obtained by using the dynamic yield stress, for which a general equation (Eq. 2.3) was developed to provide good predictions for the dynamic yield stresses in both tension and compression.

C. UMR Study - Hybrid Members

a. 19th Progress Report (B19) - Study of the Effect of Strain Rate on the Structural Strength and Crushing Behavior of Hybrid Stub Columns Using 25AK and 50SK Sheet Steels

Prior to December 1992, the UMR research work dealt only with the structural strength of cold-formed steel homogeneous members which were fabricated from or assembled with the same material in a given section. Since 1993, the study was concentrated on the strength of the hybrid sections using two different sheet steels in a built-up member. In this investigation, the material properties of 25AK and 50SK sheet steels were determined

experimentally under the strain rates from 10^{-4} to 1.0 in./in./sec. An extensive review of literature was then conducted by C.L. Pan with an emphasis on the structural strength of hybrid members and the crushing load of stub columns. Finally, a total of 96 box-shaped stub columns (Figure 3.3 (a)) and 48 hat-shaped stub columns (Figure 3.3 (b)) were fabricated from 25AK and 50SK sheet steels and tested under dynamic loads using strain rates from 10^{-4} to 10^{-1} in./in./sec. Among these stub column tests, 80 specimens were hybrid sections.

This progress report discusses the effect of strain rate on the structural strength and crushing behavior of cold-formed steel stub columns. In the evaluation of the test data, the ultimate axial load of hybrid stub columns was calculated by using the following equation:

$$P_u = (A_e)_1 (F_y)_1 + (A_e)_2 (F_y)_2 \tag{3.25}$$

The subscripts of "1" and "2" used in Equation 3.25 represent the components in the stub column fabricated from two different sheet steels. The effective design widths to be used for determining the effective cross-sectional areas, $(A_e)_1$ and $(A_e)_2$, were computed on the basis of $(F_y)_1$ and $(F_y)_2$, respectively. It should be noted that Equation 3.25 can be used to compute the ultimate axial load for hybrid sections only if the slenderness ratio of the column is small to avoid overall buckling of the member.

As far as the mean crushing load is concerned, the following empirical equation was developed for predicting the mean crushing load by using the computed ultimate load for box-shaped and hat-shaped stub columns failed by folding:

$$P_{mean} = [0.141\ (\alpha - 1.144) + 0.361]P_u \tag{3.26}$$

where α = aspect ratio, d'/b', as defined in Figure 3.4. The mean crushing load computed according to Equation 3.26 was based on the computed ultimate load according to Equation 3.25 using the dynamic yield stress corresponding to the strain rate used in the tests.

Consequently, the following additional conclusions were drawn from this investigaton for hybrid stub columns (B19 and D13):

1. Better predictions of the ultimate capacity can be achieved by using dynamic tensile yield stresses for both box-shaped and hat-shaped hybrid stub columns fabricated from 25AK and 50SK sheet steels.
2. Equation 3.25 can be used for the prediction of the ultimate axial load for hybrid stub columns fabricated from 25AK and 50SK sheet steels, provided that the overall column buckling does not occur.
3. In addition to the effect of cold-work of forming, the tested loads are also affected by the type of stress-strain relationship of the material.
4. The percentage increases in mean crushing loads are found to be slightly less than the percentage increases in ultimate loads for the stub column specimens used in this investigation.
5. The box-shaped stub columns fabricated from 50SK sheet steel are less strain-rate sensitive than those fabricated from the 25AK sheet steel for ultimate loads and mean crushing loads.
6. For design purposes, the mean crushing loads may be estimated by using the computed ultimate load (Eq. 3.25) in Equation 3.26. For box-shaped and hat-

shaped stub columns, the utlimate loads were calculated on the basis of dynamic tensile yield stresses.

b. 20th Progress Report (B20) - Study of the Effect of Strain Rate on the Bending Strength of Hybrid Beams Using 25AK and 50SK Sheet Steels

The study of hybrid beams fabricated from 25AK and 50SK sheet steels was initiated at UMR in October 1993. A total of 72 hat-shaped beams (Figure 3.5) were tested under strain rates from 10^{-4} to 10^{-2} in./in./sec.

Because 50SK sheet steel has a sharp-yielding stress-strain curve and 25AK sheet steel has a gradual-yielding stress-strain curve, the conventional method for determining the bending ultimate strength of homogeneous beams may not apply directly to hybrid beams using both 25AK and 50SK sheet steels. For this reason, a different design procedure was used in the evaluation of test data by applying the actual stress-strain relationships derived from material tests. Conclusions for the effect of strain rate on the bending capacity of hybrid beam sections were presented in the 20th Progress Report.

In the determination of yield moment, the following design approach was used in the evaluation of test data. (B20).

- For the case of initiation of yielding occuring in the top compression flange of the hybrid beam:
  1. The section is sub-divided into a number of elements (a total of 12 segments were used in the calculation).
  2. A position of the neutral axis is assumed and the strain in the top fiber of the

compression flange is assumed to be the yield strain of the steel used. From the distance between the top fiber and the neutral axis and the yield strain, the average strains in various elements are calculated.

3. From the tested stress-strain relationship obtained from material tests, the average stresses, σ, in various elements corresponding to such computed strains are found.
4. Calculate the effective width of the compression flange according to the yield stress of the steel in the compression flange.
5. Compute the area (dA) for each element and use the effective section of the compression flange.
6. The neutral axis can be located by iteration to satisfy the condition that $\Sigma dA\sigma = 0$.
7. The computed yield moment of a hybrid beam can be calculated by multiplying the force ($dA\sigma$) by the distance from the neutral axis for each element and summing up these values ($\Sigma dA\sigma y$), in which y is the distance measured from the neutral axis to the centroid of each element.

- For the case of initiation of yielding occuring in the bottom tension flange of the hybrid beam, the yield moment can be computed by using the same steps discussed above except that steps (2) and (4) are changed as follows:

2. A position of the neutral axis is assumed and the strain in the bottom fiber of the tension flange is assumed to be the yield strain of the steel used. From to these two values, the average strains in various elements are calculated.
4. Calculate the effective width of the stiffened compression flange for the compression stress obtained from the yield strain of the steel in the tension flange and the assumed neutral axis.

For the determination of the ultimate moment, the inelastic reserve capacity of flexural members may be used to allow partial plastification of the cross-section, provided that such members satisfy the specific requirements. However, the design procedures recommended in the Automotive Steel Design Manual (A2) may not be used directly to compute the ultimate flexural strength for the test specimens studied in this investigation, because the beam specimens were fabricated from two different sheet steels with different types of stress-strain curves. For this reason, the ultimate moments of hybrid beams were computed on the basis of the stress-strain diagrams given in this report for four different groups of cross sections.

Based on the evaluation of available test data, the following conclusions were drawn in the 20th Progress Report for the hybrid beams fabricated from 25AK and 50SK sheet steels:

- For most cases, the yield moment of hybrid beams increase with increasing strain rate for specimens having the similar w/t ratios.
- The dynamic material properties can be used for the calculation of yield moment

of hybrid beams. The computed yield moments calculated on the basis of the dynamic tensile stresses are less conservative than those calculated on the basis of the dynamic compressive stresses.

- The calculation procedures presented in the 20th Progress Report give reasonable results for the yield moment of hybrid beams.
- The dynamic stress-strain relationship can also be used for calculating the ultimate moment of hybrid beams. The measured or estimated strain under the ultimate load is needed for computing the ultimate moment for hybrid sections.
- The effective cross-sectional area determined according to the Automotive Steel Design Manual (A2) can also be used in the calculation of yield moment and ultimate moment for hybrid sections.
- For hybrid beams fabricated from gradual-yielding type of material, the calculation of ultimate moments may use a stress higher than the yield point in order to consider the inelastic reserve capacity.

c. 21st Progress Report (B21) - Aging Effect on the Yield Moment of Hybrid Beams

The aging effect on the mechanical properties of 25AK and 50SK sheet steels was discussed in the 21st Progress Report and was summarized in Section II.E of this report. In order to study the changes of the computed yield moments as affected by the increases of the yield stress due to the aging effect, the yield moments of six hybrid beams were recomputed by using the dynamic tensile yield stresses interpolated from Figures 2.23 and 2.24 for the time of beam tests. These recomputed yield moments were compared with the original

values presented in the 20th Progress Report. It was found that the aging effect on the bending capacity of hybrid beams is slightly less than the aging effect on material properties of steel.

d. 22nd Progress Report (B22) - Transformed Section Method for the Calculation of Yield Moment of Hybrid Beams

In the 20th Progress Report, the yield moment of hybrid beams was determined by an iterative design procedure using the stress-strain relationships obtained from material tests. This was because the hybrid beams used for the tests were fabricated from two different sheet steels, for which 50SK sheet steel had a sharp-yielding stress-strain curve and 25AK sheet steel had a gradual-yielding stress-strain curve (Figure 3.6).

For the purpose of simplifying the design procedure, the Transformed Section Method is discussed in the 22nd Progress Report for the calculation of yield moment of hybrid beams by using the simulated stress-strain relationships as shown in Figure 3.7. When using this method, the yield stress, proportional limit, yield strain, and the strain for proportional limit of each material must be known from the coupon tests. Otherwise, if the stress-strain curves of both 50SK and 25AK sheet steels were assumed to be sharp-yielding type, at the respective F_y values, the calculations presented in the 20th Progress Report indicated that the computed moment would be conservative as compared with the tested value, particularly for the beams with small w/t ratios.

D. GM Study - Hybrid Stub Columns

A total of 70 stub column tests were conducted in General Motors Corporation using

homogeneous and hybrid sections. Among these tests, 52 specimens were tested by using a drop silo test facility and 18 specimens were tested for the quasi-static condition. Seven types of stub column specimens were used in the GM tests. The selected speeds used for the tests were 43.2, 28.5, and 1.524×10^{-3} km/hr (B19). Test results indicate that the ultimate load, energy absorption, and mean crushing load were affected by the loading rate, type of steel for individual components, and cross-sectional geometry of the stub columns. Graphical comparisons of the GM and UMR tested mean crushing loads for box-shaped stub columns are shown in Figures 3.8 and 3.9. In Figure 3.8, specimens A1, B1, and C1 are the box-shaped hybrid stub columns (Figure 3.3a) with relatively small width-to-thickness ratios for compression flanges. For stub columns A3, B3, and C3 with relatively large width-to-thickness ratios, the mean crushing loads are shown in Figure 3.9. Figure 3.10 shows the mean crushing loads for hat-shaped stub columns D1 and E1 (Figure 3.3b) with small width-to-thickness ratios. Numerical comparisons of the tested and predicted mean crushing loads of box-shaped and hat-shaped stub columns were presented in Tables 4.21 through 4.25 of the 19th Progress Report (B19). It was reported that the ratios of the tested-to-predicted mean crushing loads range from 0.84 to 1.27 for the GM and UMR tests.

The research findings obtained from the GM tests were presented by Schell et al. and Pan et al. in two conference papers (D17 and D13). Based on the 19th Progress Report, Reference D13 concludes that the ultimate loads and mean crushing loads of cold-formed steel stub columns increase with increasing strain rates. Better prediction of ultimate loads can be obtained by using the dynamic yield stresses. The effective cross-sectional area can also be employed in the calculation of ultimate loads for hybrid sections. Equation 3.26 can

be used for computing the mean crushing loads of box-shaped and hat-shaped stub columns failed by folding. It can be used only for the stub columns having the aspect ratio between 0.5 and 2.0 with sufficient connectors to prevent premature failure.

IV. SUMMARY

This report summarizes the research work on automotive components conducted at the University of Missouri-Rolla during the period from 1988 through 1997 under the sponsorship of the American Iron and Steel Institute. The primary goals of this phase of the overall project were to investigate the effect of strain rate on material properties and the structural strength of cold-formed steel homogeneous and hybrid members and to determine whether the AISI design formulas originally developed from the static loads can also be used for structural members subjected to dynamic loads. The research findings presented herein are based on 12 progress reports, (B11-B22) two theses, (C4 and C5), and 10 journal and conference papers (D9-D18). Details of the test results with evaluations are given in the cited references.

A. Effect of Strain Rate on Material Properties

A total of five types of sheet steels with nominal yield stresses from 25 to 100 ksi have been selected to study the effect of strain rate on material properties. The research findings are summarized in this report. For design purpose, the tensile and compressive yield stresses can be estimated by using Equation 2.3 for the strain rates from 10^{-4} to 10^{2} in./in./sec. allowing some extrapolation of the test data as discussed in Section II.D.b.

B. Effect of Strain Rate on the Structural Strength of Cold-Formed Steel Members

In Section III of this report, the UMR research work for the effect of strain rate on the structural strength of cold-formed steel stub columns and flexural members were summarized according to the sequence of progress reports. The strength and behavior of stub

columns and beams are briefly discussed in subsequent subsections.

a. Homogeneous Stub columns

For the homogeneous stub columns which were fabricated from the same material in a given member, conventional equations (Eqs. 3.1 and 3.2) were used to determine the critical local buckling load and the ultimate axial load. The load-displacement relationship of stub columns depends on (1) the type of the controlling compression element, i.e., stiffened or unstiffened, (2) the width-to-thickness ratio, w/t, of the controlling compression element, (3) the stress-strain relationship of the material, i.e., sharp-yielding or gradual yielding, and (4) the strain rate used for the test. Figures 3.11 through 3.26 show graphically the differences between the load-displacement relationships for stub columns using 35XF and 50XF sheet steels. In these figures, Figures 3.11 through 3.18 are load-displacement curves for box-shaped stub columns, for which the strength was controlled by stiffened compression elements, while Figures 3.19 through 3.26 are dealing with I-shaped stub columns, for which the strength was governed by unstiffened compression elements.

b. Homogeneous Beams

For the homogeneous beams using the same material in a given section, Equations 3.3, 3.4, and 3.6 were used to compute the critical local buckling moment, yield moment, and ultimate moment, respectively. Figures 3.27 through 3.31 illustrate the load-displacement relationships of hat-shaped beams having stiffened compression flanges, while Figures 3.32 through 3.37 show the load-displacement curves for channel beams having unstiffened

compression flanges.

c. Hybrid Stub Columns

For hybrid stub columns using two different sheet steels in a given section, Equations 3.25 and 3.26 were used to compute the ultimate axial load and the mean crushing load, respectively. Figure 3.38 shows a typical load-displacement curve of a hybrid stub column having a total displacement of five inches.

d. Hybrid Beams

Because of the use of two different sheet steels in a given section, the conventional method for computing the bending moment of homogeneous beams may not be used directly for hybrid beams. An iterative procedure was used in the 20th Progress Report for the evaluation of the bending capacity. The load-displacement relationships were found to be affected by the beam composition and configuration, strain rate, and the width-to-thickness ratio of the compression flange.

e. Conclusions

In summary, the following combined conclusions were drawn for the design of compression and flexural members subjected to dynamic loads:

1. For most of the member tests, the critical local buckling strength, yield strength, and ultimate strength increased with increasing strain rates.
2. The effect of strain rate on member strength was found to be slightly higher than that

for material properties. This may be partially due to the increase of yield strength due to aging effect.

3. The ultimate strength computed in accordance with the Automotive Steel Design Manual was found to be conservative as compared with the test results of stub columns and beams. The prediction of the ultimate capacity was improved by using the dynamic yield stress.

4. For stub columns and beams having small w/t ratios, a better prediction of the strength can usually be achieved by considering the cold-work of forming, provided that the specific requirements of the AISI Specification (A1) are met.

5. The computed moments for the beams fabricated from 50XF sheet steel were found to be less conservative than the beams fabricated from 35XF sheet steel.

6. The computed ultimate moments for beams having stiffened flanges were less conservative than the beams having unstiffened flanges.

7. For noncompact stub columns and beams having unstiffened compression elements, Kalyanaraman's equations can be used for determining local buckling coefficients.

8. For hybrid stub columns, Equation 3.7 can be used to predict the ultimate load, provided that the overall member buckling does not occur. The mean crushing load can be estimated by applying Equation 3.8.

9. An iterative design procedure can be used to compute the yield moment of hybrid beams as illustrated in the 20th Progress Report by using the actual stress-strain relationships obtained from material tests. The Transformed Section Method is discussed in the 22nd Progress Report by using the simulated stress-strain

relationships of sheet steels.

10. The aging effect on material properties may have a minor influence on the structural strength of automotive components cold-formed to shape from sheet steels. However, the equations developed from this investigation and the conclusions drawn from this study are applicable to the design of automotive components whether or not the aging effect on material properties is considered.

REFERENCES

A. General

1. American Iron and Steel Institute (1980, 1986), *Specification for the Design of Cold-Formed Steel Structural Members*, 1980 edition and 1986 edition.

2. American Iron and Steel Institute (1996), *Automotive Steel Design Manual*, Revision 5, May 1996.

B. Research Reports

1. Yu, W.W., Santaputra, C. and Parks, M.B. (1983), "Design of Automotive Structural Components Using High Strength Sheet Steels," 1st Progress Report, Civil Engineering Study 83-1, University of Missouri-Rolla, January 1983.

2. Parks, M.B. and Yu, W.W. (1983a), "Design of Automotive Structural Components Using High Strength Sheet Steels: Mechanical Properties of Materials," 2nd Progress Report, Civil Engineering Study 83-3, University of Missouri-Rolla, August 1983.

3. Santaputra, C. and Yu, W.W. (1983), "Design of Automotive Structural Components Using High Strength Sheet Steels: Strength of Beam Webs," 3rd Progress Report, Civil Engineering Study 83-4, University of Missouri-Rolla, August 1983.

4. Parks, M.B. and Yu, W.W. (1983b), "Design of Automotive Structural Components Using High Strength Sheet Steels: Preliminary Study of Members Consisting of Flat and Curved Elements," 4th Progress Report, Civil Engineering Study 83-5, University of Missouri-Rolla, August 1983.

5. Santaputra, C. and Yu, W.W. (1984), "Design of Automotive Structural Components Using High Strength Sheet Steels: Structural Behavior of Beam Webs Subjected to Web Crippling and a Combination of Web Crippling and Bending," 5th Progress Report, Civil Engineering Study 84-1, University of Missouri-Rolla, October 1984.

6. Parks, M.B. and Yu, W.W. (1984), "Design of Automotive Structural Components Using High Strength Sheet Steels: Status Report on the Study of Members Consisting of Flat and Curved Elements," 6th Progress Report, Civil Engineering Study 84-2, University of Missouri-Rolla, October 1984.

7. Parks, M.B. and Yu, W.W. (1985), "Design of Automotive Structural Components Using High Strength Sheet Steels: Results and Evaluation of Stub Column Tests for Unstiffened Curved Elements," 7th Progress Report, Civil Engineering Study 85-1, University of

Missouri-Rolla, September 1985.

8. Santaputra, C. and Yu, W.W. (1986), "Design of Automotive Structural Components Using High Strength Sheet Steels: Web Crippling of Cold-Formed Steel Beams," 8th Progress Report, Civil Engineering Study 86-1, University of Missouri-Rolla, August 1986.

9. Parks, M.B. and Yu, W.W. (1987), "Design of Automotive Structural Components Using High Strength Sheet Steels: Structural Behavior of Members Consisting of Flat and Curved Elements," 9th Progress Report, Civil Engineering Study 87-2, University of Missouri-Rolla, June 1987.

10. Lin, S.H., Hsiao, L.E., Pan, C.L. and Yu, W.W. (1988), "Design of Automotive Structural Components Using High Strength Sheet Steels: Structural Strength of Cold-Formed Steel I-Beams and Hat Sections Subjected to Web Crippling Load," 10th Progress Report, Civil Engineering 88-5, University of Missouri-Rolla, June 1988.

11. Kassar, M. and Yu, W.W. (1989a), "Design of Automotive Structural Components Using High Strength Sheet Steels: The Effect of Strain Rate on Mechanical Properties of Sheet Steels," 11th Progress Report, Civil Engineering Study 89-2, University of Missouri-Rolla, January 1989.

12. Kassar, M. and Yu, W.W. (1989b), "Design of Automotive Structural Components Using High Strength Sheet Steels: The Effect of Strain Rate on Mechanical Properties of Sheet Steels," 12th Progress Report, Civil Engineering Study 89-4, University of Missouri-Rolla, August 1989.

13. Kassar, M. and Yu, W.W. (1990a), "Design of Automotive Structural Components Using High Strength Sheet Steels: Structural Strengths of Cold-Formed Steel Members under Dynamic Loads," 13th Progress Report, Civil Engineering Study 90-1, University of Missouri-Rolla, May 1990.

14. Kassar, M. and Yu, W.W. (1990b), "Design of Automotive Structural Components Using High Strength Sheet Steels: Effect of Strain Rate on Material Properties of Sheet Steels and Structural Strengths of Cold-Formed Steel Members," 14th Progress Report, Civil Engineering Study 90-2, University of Missouri-Rolla, May 1990.

15. Pan, C.L. and Yu, W.W. (1990), "Design of Automotive Structural Components Using High Strength Sheet Steels: Structural Strength of Cold-Formed Steel Members under Dynamic Loads," 15th Progress Report, Civil Engineering Study 90-3, University of Missouri-Rolla, November 1990.

16. Pan, C.L. and Yu, W.W. (1991), "Design of Automotive Structural Components Using High Strength Sheet Steels: Structural Strength of Cold-Formed Steel Beams under Dynamic

Loads," 16th Progress Report, Civil Engineering Study 91-4, University of Missouri-Rolla, September 1991.

17. Pan, C.L. and Yu, W.W. (1992a), "Design of Automotive Structural Components Using High Strength Sheet Steels: Mechanical Properties of Materials," 17th Progress Report, Civil Engineering Study 92-2, University of Missouri-Rolla, May 1992.

18. Pan, C.L. and Yu, W.W. (1992b), "Design of Automotive Structural Components Using High Strength Sheet Steels: Influence of Strain Rate on the Mechanical Properties of Sheet Steels and Structural Performance of Cold-Formed Steel Members," 18th Progress Report, Civil Engineering Study 92-3, University of Missouri-Rolla, December 1992.

19. Pan, C.L. and Yu, W.W. (1993), "Design of Automotive Structural Components Using High Strength Sheet Steels: Effect of Strain Rate on the Structural Strength and Crushing Behavior of Cold-Formed Steel Stub Columns," 19th Progress Report, Civil Engineering Study, 93-1, University of Missouri-Rolla, July 1993.

20. Pan, C.L. and Yu, W.W. (1995), "Design of Automotive Structural Components Using High Strength Sheet Steels: Effect of Strain Rate on the Structural Strength of Cold-Formed Steel Hybrid Beams," 20th Progress Report, Civil Engineering Study 95-4, University of Missouri-Rolla, June 1995.

21. Wu, S, Pan, C.L. and Yu, W.W. (1997), "Design of Automotive Structural Components Using High Strength Sheet Steels: Mechanical Properties of Materials (Aging Effect)," 21st Progress Report, Civil Engineering Study 97-1, University of Missouri-Rolla, January 1997.

22. Pan, C.L. and Yu, W.W. (1997), "Design of Automotive Structural Components Using High Strength Sheet Steels: Transformed Section Methods for the Calculation of Yield Moment of Cold-Formed Steel Hybrid Beams," 22nd Progress Report, Civil Engineering Study 98-1, University of Missouri-Rolla, February 1998.

C. **Theses**

1. Santaputra, C. (1986), "Web Crippling of Cold-Formed Steel Beams," Ph.D. Thesis, 1986.

2. Parks, M.B. (1987), " Structural Behavior of Members Consisting of Flat and Curved Elements," Ph.D. Thesis, 1987.

3. Pan, L.C. (1987), "Effective Widths of High Strength Cold-Formed Steel Members," Ph.D. Thesis, 1987.

4. Kassar, M. (1990), "Effect of Strain Rate on Material Properties of Sheet Steels and Structural Strengths of Cold-Formed Steel Members," Ph.D. Thesis, 1990.

5. Pan, C.L. (1992), "Influence of Strain Rate on the Mechanical Properties of Sheet Steels and Structural Performance of Cold-Formed Steel Members," Ph.D. Thesis, 1992.

D. Journal and Conference Papers

1. Parks, M.B., Santaputra, C. and Yu, W.W. (1986a), "Structural Behavior of Members Consisting of Curved Elements," *Proceedings of the Sixth International Conference on Vehicle Structural Mechanics*, April 1986.

2. Santaputra, C., Parks, M.B. and Yu, W.W. (1986a), "Web Crippling of Cold-Formed Steel Beams Using High Strength Sheet Steels," *Proceedings of the Sixth International Conference on Vehicle Structural Mechanics*, April 1986.

3. Parks, M.B., Santaputra, C. and Yu, W.W. (1986b), "Local Buckling of Curved Elements," *Proceedings of the Eighth International Specialty Conference on Cold-Formed Steel Structures*, University of Missouri-Rolla, November 1986.

4. Santaputra, C., Parks, M.B. and Yu, W.W. (1986b), "Web Crippling Strength of High Strength Steel Beams," *Proceedings of the Eighth International Specialty Conference on Cold-Formed Steel Structures*, University of Missouri-Rolla, November 1986.

5. Parks, M.B. and Yu, W.W. (1987), "Structural Behavior of Members Consisting of Flat and Curved Elements," *Proceedings of the SAE International Congress and Exposition.* February, 1987.

6. Pan, L.C. and Yu, W.W. (1988), "High Strength Steel Members with Unstiffened Compression Elements," *Proceedings of the Ninth International Specialty Conference on Cold-Formed Steel Structures*, University of Missouri-Rolla, November 1988.

7. Parks, M.B. and Yu, W.W. (1989), "Local Buckling Behavior of Stiffened Curved Elements," *International Journal on Thin-Walled Structures*, Vol. 7, No. 1, Elsevier Applied Science, London, U.K., 1989.

8. Santaputra, C., Parks, M.B. and Yu, W.W. (1989), "Web Crippling Strength of Cold-Formed Steel Beams," *Journal of Structural Engineering*, ASCE, Vol. 115, No. 10, October, 1989.

9. Kassar, M. and Yu, W.W. (1990), "Effect of Strain Rate on Cold-Formed Steel Stub Columns," *Proceedings of the Tenth International Specialty Conference on Cold-Formed Steel Structures*, University of Missouri-Rolla, October 1990.

10. Kassar, M. and Yu, W.W. (1992), "Effect of Strain Rate on Cold-Formed Steel Stub Columns,"*Journal of Structural Engineering,* ASCE, Vol. 118, No.11, November 1992.

11. Pan, C.L., Kassar, M., and Yu, W.W. (1992), "Effect of Strain Rate on Material Properties of Sheet Steels," *Journal of Structural Engineering*, ASCE, Vol. 118, No. 11, November 1992.

12. Pan, C.L. and Yu, W.W. (1993), "Influence of Strain Rate on the Structural Strength of Cold-Formed Steel Automotive Components," *Proceedings of Automotive Body Materials of the International Body Engineering Conference*, Detroit, Michigan, September 1993.

13. Pan, C.L., Yu, W.W., Schell, B.C., and Sheh, M.Y. (1994), "Effect of Strain Rate on the Structural Strength and Crushing Behavior of Hybrid Stub Columns," *Proceedings of the International Body Engineering Conference,* Detroit, Michigan, September 1994.

14. Pan, C.L. and Yu, W.W. (1995), "Mechanical Properties of Sheet Steels and Structural Strength of Cold-Formed Steel Stub Columns Affected by Strain Rate," *Proceedings of the 4th Pacific Structural Steel Conference,* Singapore, October 1995.

15. Pan, C.L. and Yu, W.W. (1995), "Structural Strength and Crushing Behavior of Hybrid Cold-Formed Steel Stub Columns under Dynamic Loading Condition," *Proceedings of the International Conference on Structural Stability and Design*, Sydney, Australia, November 1995.

16. Pan, C.L. and Yu, W.W. (1996), "Structural Strength of Hybrid Cold-Formed Steel Beams under Dynamic Loading Condition," *Proceedings of the Body Design and Engineering of the International Body Engineering Conference,* Detroit, Michigan, September 1996.

17. Schell, B.C., Sheh, M.Y., Tran, P.H., Pan, C.L., and Yu, W.W. (1993), "Impact and Static Crush Performance of Hybrid Hat Section Stub Columns," *Proceedings of Automotive Body Design and Engineering of the International Body Engineering Conference,* Detroit, Michigan, September 1993.

18. Yu, W.W., Parks, M.B., Santaputra, C., Pan, L.C., Kassar, M., and Pan, C.L. (1993), "Automotive Structural Components Using High Strength Sheet Steels," *International Workshop on Cold-Formed Steel Structures,* Sydney, Australia, February 1993.

Table 2.1

Average Tensile Mechanical Properties of Sheet Steels
Longitudinal Tension, Virgin Material

AISI Designation	Strain Rate in./in./sec.	F_y (ksi)	F_u (ksi)	Elongation (percent)	Reference Report
35XF	0.0001	32.87	49.35	38.9	B11, B14, B18
	0.01	36.40	51.76	36.8	
	1.0	42.37	56.63	40.9	
50XF	0.0001	49.50	72.97	31.0	B11, B14, B18
	0.01	51.60	74.87	27.0	
	1.0	54.66	78.73	25.8	
100XF	0.0001	124.25	124.25	9.5	B11, B14, B18
	0.01	125.80	125.80	10.2	
	1.0	128.91	128.91	---	
25AK	0.0001	24.60	42.76	---	B17, B18
	0.01	27.86	44.44	49.31	
	1.0	35.13	51.25	58.18*	
50SK	0.0001	54.97	67.07	36.09	B17, B18
	0.01	56.83	68.98	33.34	
	1.0	60.73	76.50	40.13	

* Because the maximum range for the extensometer is 1.0 inch, this elongation was measured from the distance between the gage marks of tension coupons.

Table 2.2

Average Compressive Mechanical Properties of Sheet Steels
Longitudinal Compression, Virgin Material

AISI Designation	Strain Rate in./in./sec.	F_{pr} (ksi)	F_y (ksi)	F_{pr}/F_y	Reference Report
35XF	0.0001	17.79	29.83	0.60	B12, B14, B18
	0.01	20.03	31.92	0.63	
	1.0	-----	36.91	-----	
50XF	0.0001	38.64	49.68	0.78	B12, B14, B18
	0.01	40.05	52.51	0.76	
	1.0	-----	54.79	-----	
100XF	0.0001	71.25	107.29	0.66	B12, B14, B18
	0.01	88.44	111.26	0.79	
	1.0	-----	114.91	------	
25AK	0.0001	15.93	21.66	0.74	B17, B18
	0.01	19.55	24.77	0.79	
	1.0	-----	38.14	-----	
50SK	0.0001	41.98	53.35	0.79	B17, B18
	0.01	42.46	55.91	0.76	
	1.0	-----	59.41	-----	

Table 2.3

Comparison of Mechancial Properties of 25AK and 50SK

Sheet Steels in Longitudinal Tension for Aging and Strain Rate Effect

Sheet Steel	Strain Rate (in./in./sec.)	Yield Strength Ratio		Tensile Strength Ratio
		$F_{y,95} / F_{y,92}$	$F_{y,97} / F_{y,92}$	$F_{u,97} / F_{u,92}$
25AK	0.0001	1.09	1.06	1.05
50SK	0.0001	1.06	1.05	1.04
25AK	0.01	-	1.10	1.10
50SK	0.01	-	1.07	1.04

Table 2.4

Percentage Increase in Yield Stress

when the Strain Rate Increases from 0.0001 to 1.0 in./in./sec.

AISI Designation	Longitudinal Tension	Longitudinal Compression
35XF	29%	24%
50XF	10%	10%
100XF	4%	7%
25AK	43%	76%
50SK	10%	11%

Table 3.1

Comparisons of Computed and Tested Ultimate

Loads for Stub Columns Using Box-Shaped Sections

$(P_u)_{test} / (P_u)_{comp}$ Ratios

Material	Based on Static F_y		Based on Dynamic F_y	
	Mean Value	Standard Deviation	Mean Value	Standard Deviation
35XF Sheet Steel	1.222	0.149	1.148	0.105
50XF Sheet Steel	1.020	0.061	0.981	0.044

Table 3.2

Comparisons of Computed and Tested Ultimate

Loads for Stub Columns Using I-Shaped Sections

$(P_u)_{test} / (P_u)_{comp}$ Ratios

Material	Based on Static F_y		Based on Dynamic F_y	
	Mean Value	Standard Deviation	Mean Value	Standard Deviation
35XF Sheet Steel	1.410	0.132	1.330	0.067
50XF Sheet Steel	1.162	0.064	1.121	0.044

Table 3.3

Effect of Cold-Work of Forming

Comparisons of Computed and Tested Yield Moments

for Hat-Sections with a Stiffened Flange (35XF Steel)

$(M_y)_{test} / (M_y)_{comp}$ Ratios

Material	Based on Static F_y		Based on Dynamic F_y	
	Mean Value	Standard Deviation	Mean Value	Standard Deviation
Without Considering Cold -Work of Forming	1.368	0.155	1.282	0.072
Considering Cold -Work of Forming	1.141	0.130	1.082	0.072

Note: Based on Table 3.3 of the 16th Progress Report

Table 3.4

Effect of Cold-Work of Forming

Comparisons of Computed and Tested Failure Moments

for Channels with Unstiffened Flanges (35XF Steel)

$(M_u)_{test} / (M_y)_{comp}$ Ratios

Material	Based on Static F_y		Based on Dynamic F_y	
	Mean Value	Standard Deviation	Mean Value	Standard Deviation
Without Considering Cold - Work of Forming	1.365	0.098	1.281	0.051
Considering Cold - Work of Forming	1.139	0.081	1.083	0.045

Note: Based on Table 3.11 of the 16th Progress Report

Table 3.5

Comparisons of Computed and Tested Failure Moments

for Hat-Sections with a Stiffened Flange

$(M_u)_{test} / (M_y)_{comp}$ Ratios

Material	Based on Static F_y		Based on Dynamic F_y	
	Mean Value	Standard Deviation	Mean Value	Standard Deviation
35XF Sheet Metal	1.270	0.198	1.191	0.169
50XF Sheet Steel	1.063	0.075	1.036	0.063

Note: Based on Tables 3.5 and 3.6 of the 16th Progress Report.
Cold-work of forming was not considered for all specimens

Table 3.6

Comparisons of Computed and Tested Failure Moments

for Channels with Unstiffened Flanges

$(M_u)_{test} / (M_y)_{comp}$ Ratios

Material	Based on Static F_y		Based on Dynamic F_y	
	Mean Value	Standard Deviation	Mean Value	Standard Deviation
35XF Sheet Metal	1.299	0.096	1.228	0.052
50XF Sheet Steel	1.121	0.040	1.094	0.026

Note: Based on Tables 3.11 and 3.12 of the 16th Progress Report.
Cold-work of forming was not considered for all specimens.

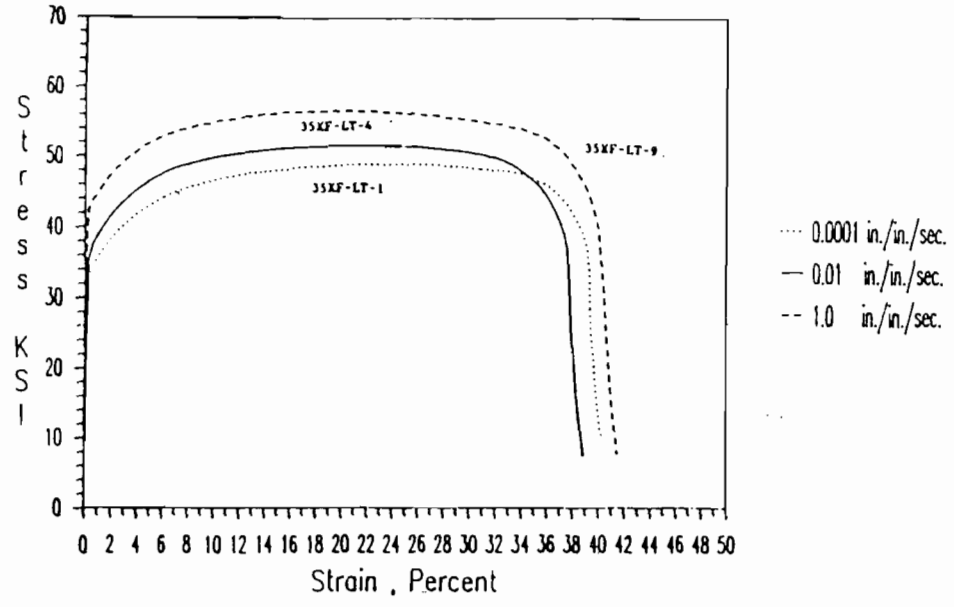

Figure 2.1 Tensile Stress-Strain Curves for 35XF-LT Steel under Different Strain Rates, Virgin Materials (B11)

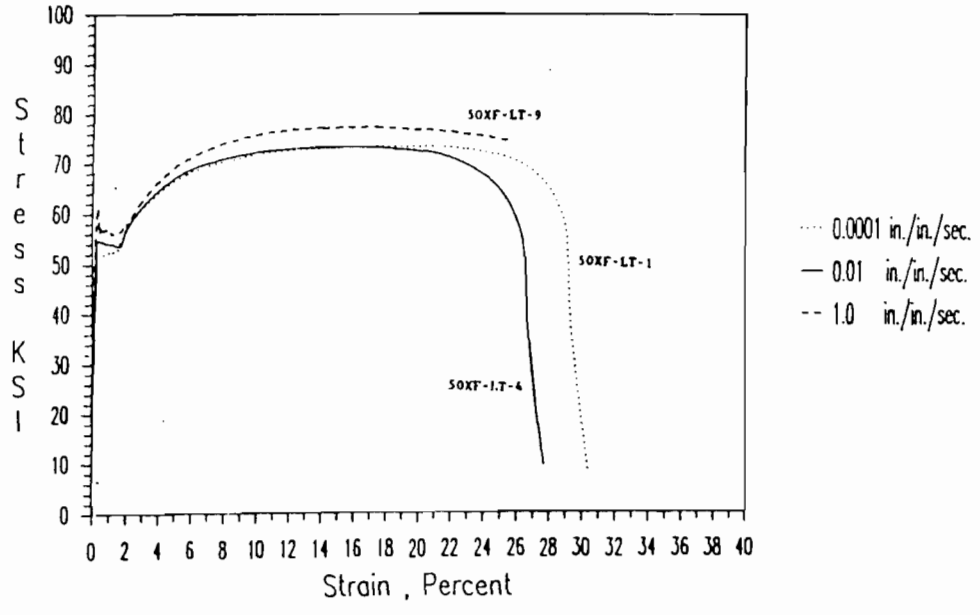

Figure 2.2 Tensile Stress-Strain Curves for 50XF-LT Steel under Different Strain Rates, Virgin Materials (B11)

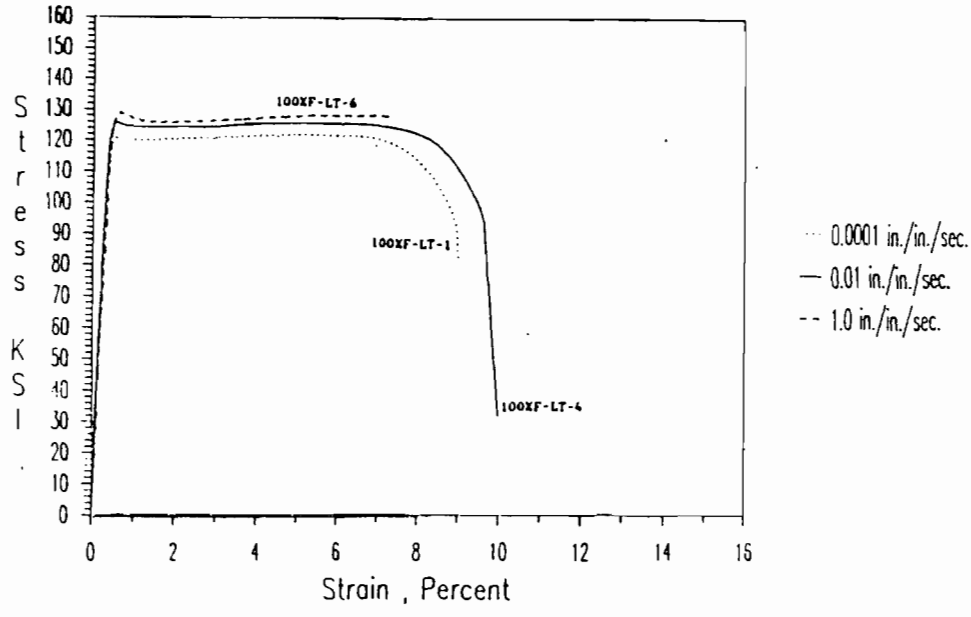

Figure 2.3 Tensile Stress-Strain Curves for 100XF-LT Steel under Different Strain Rates, Virgin Materials (B11)

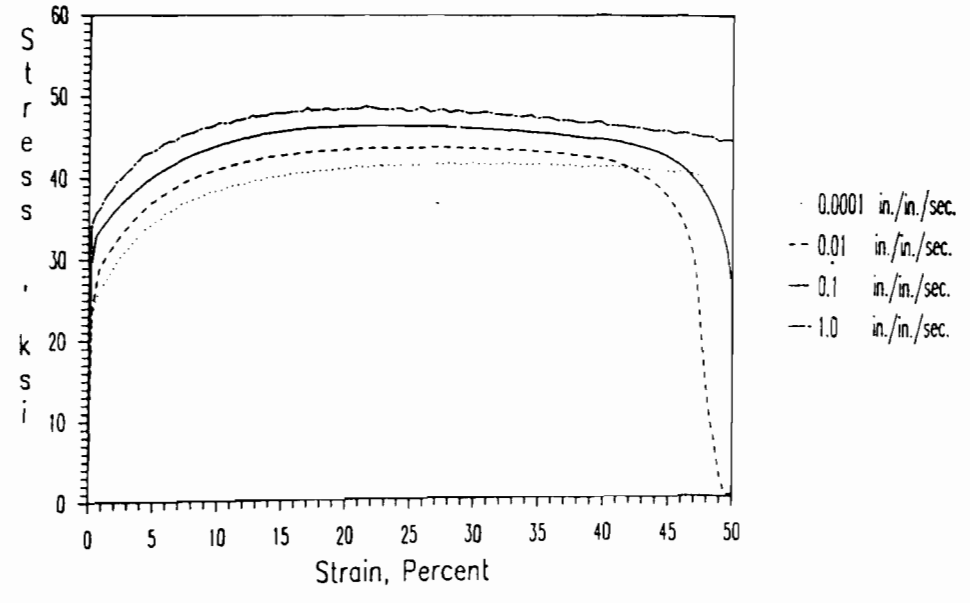

Figure 2.4 Tensile Stress-Strain Curves for 25AK-LT Steel under Different Strain Rates, Virgin Materials (B17)

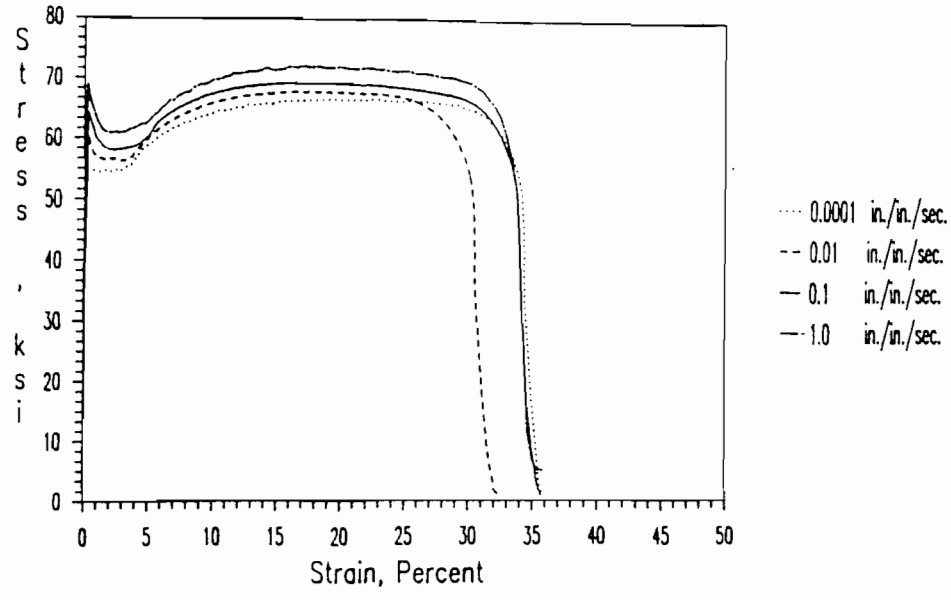

Figure 2.5 Tensile Stress-Strain Curves for 50SK-LT Steel under Different Strain Rates, Virgin Materials (B17)

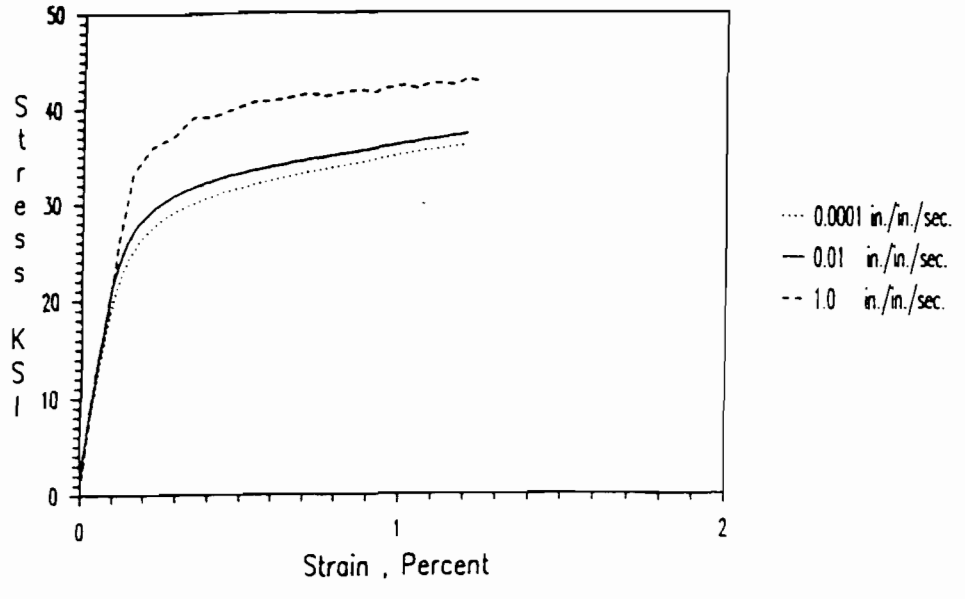

Figure 2.6 Compressive Stress-Strain Curves for 35XF-LC Steel under Different Strain Rates, Virgin Materials (B11)

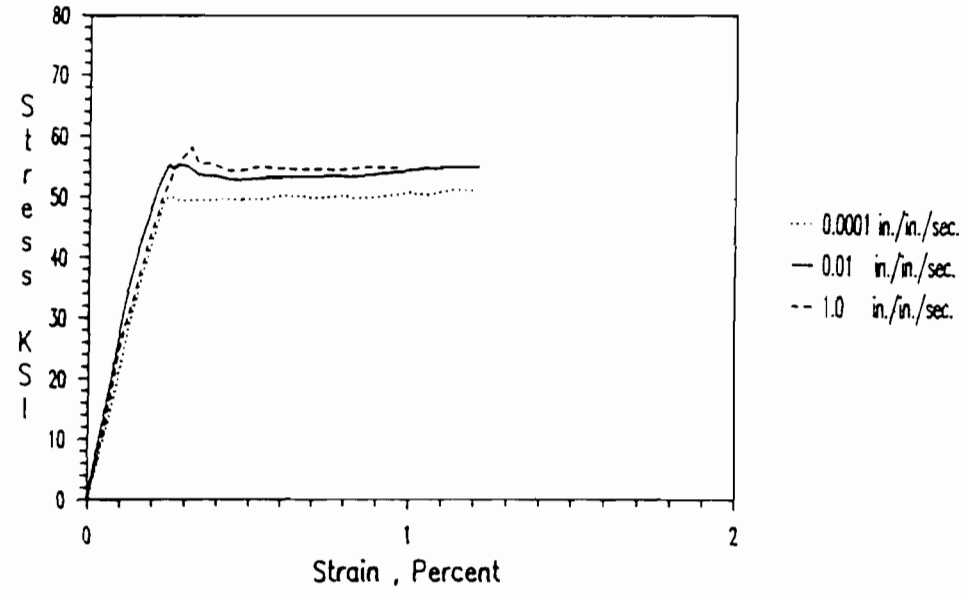

Figure 2.7 Compressive Stress-Strain Curves for 50XF·LC Steel under Different Strain Rates, Virgin Materials (B11)

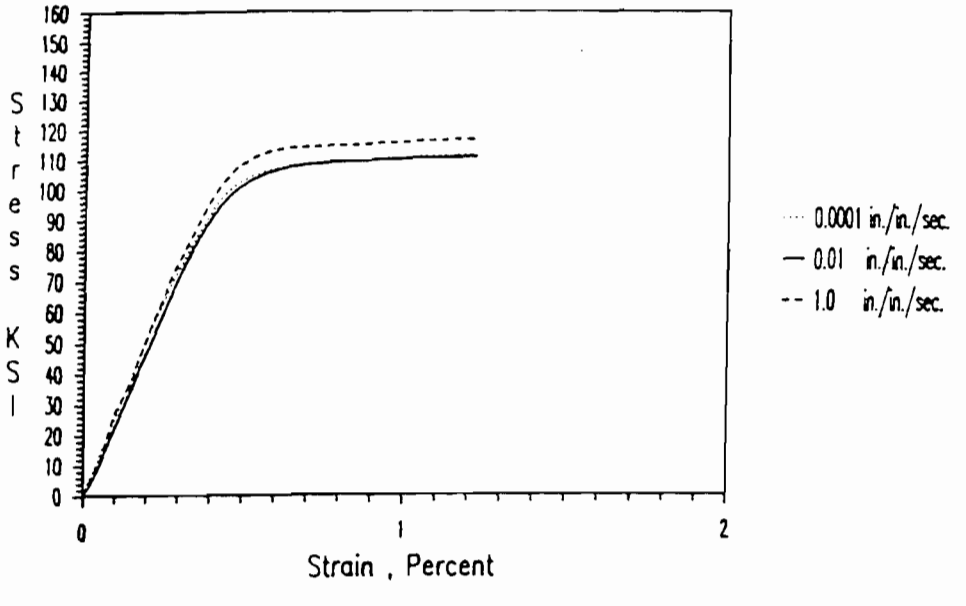

Figure 2.8 Compressive Stress-Strain Curves for 100XF·LC Steel under Different Strain Rates, Virgin Materials (B11)

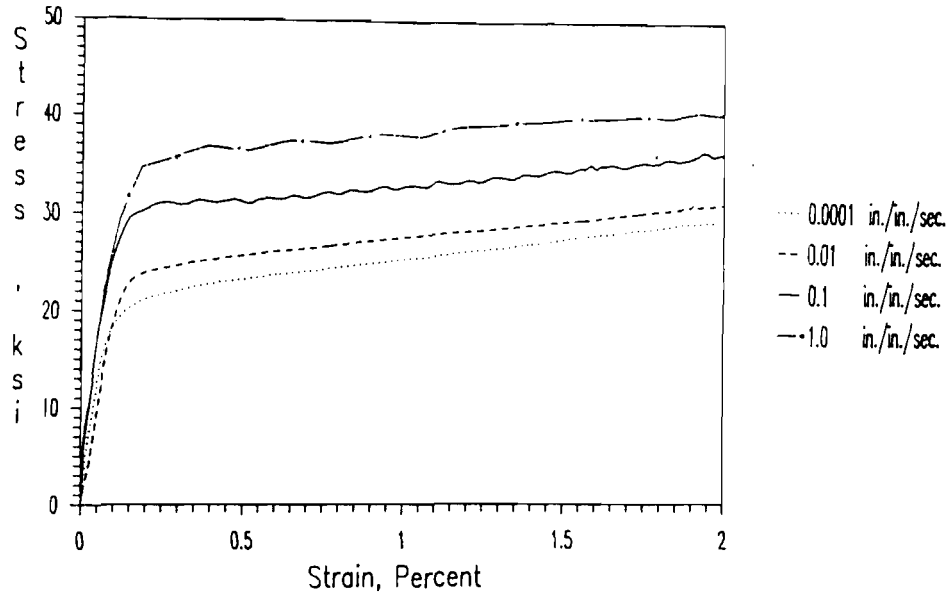

Figure 2.9 Compressive Stress-Strain Curves for 25AK-LC Steel under Different Strain Rates, Virgin Materials (B17)

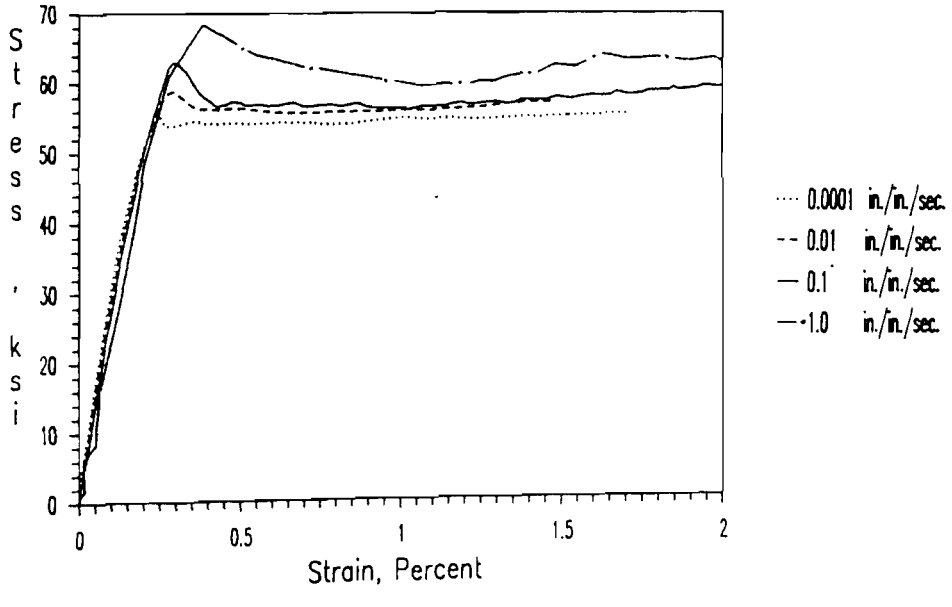

Figure 2.10 Compressive Stress-Strain Curves for 50SK-LC Steel under Different Strain Rates, Virgin Materials (B17)

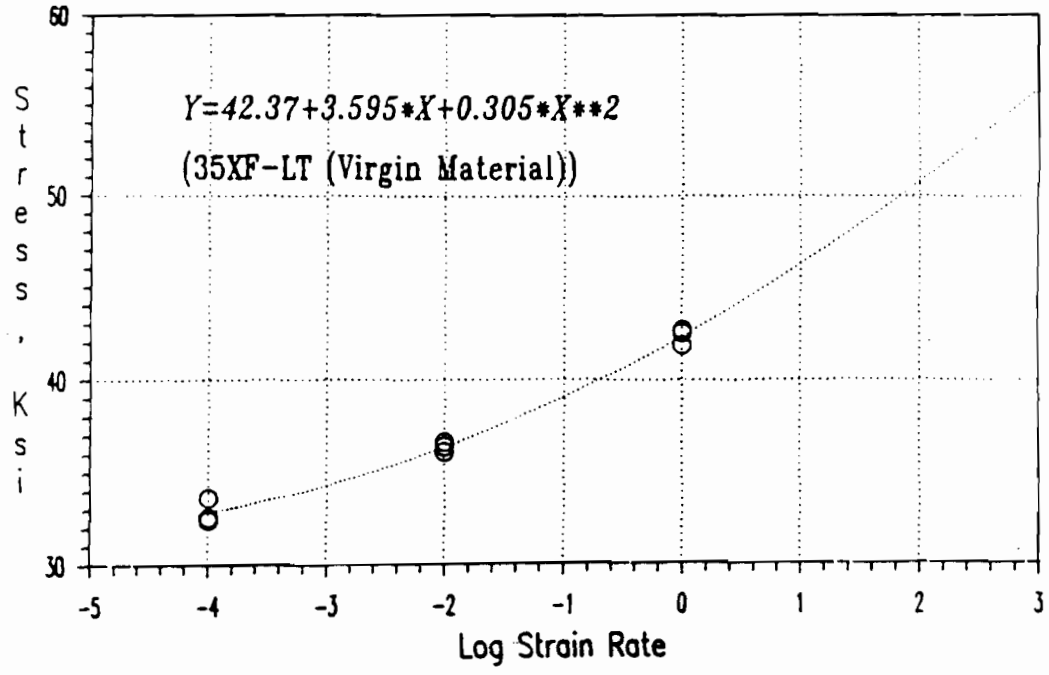

Figure 2.11 Polynomial Equation for Tensile Yield Stress of 35XF-LT Steel (B12)

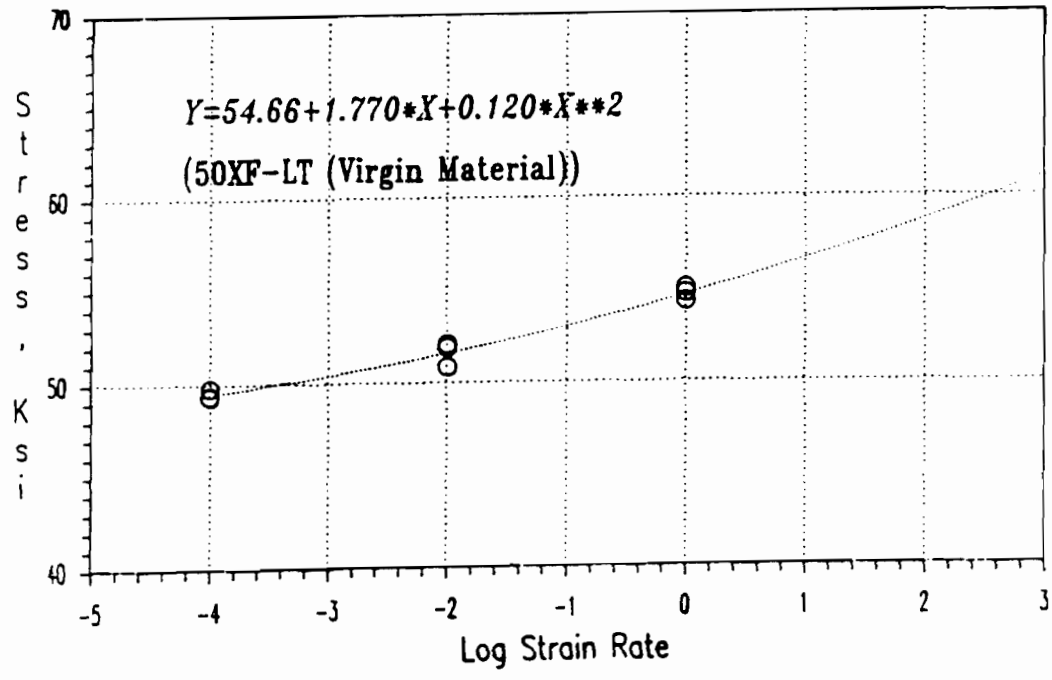

Figure 2.12 Polynomial Equation for Tensile Yield Stress of 50XF-LT Steel (B12)

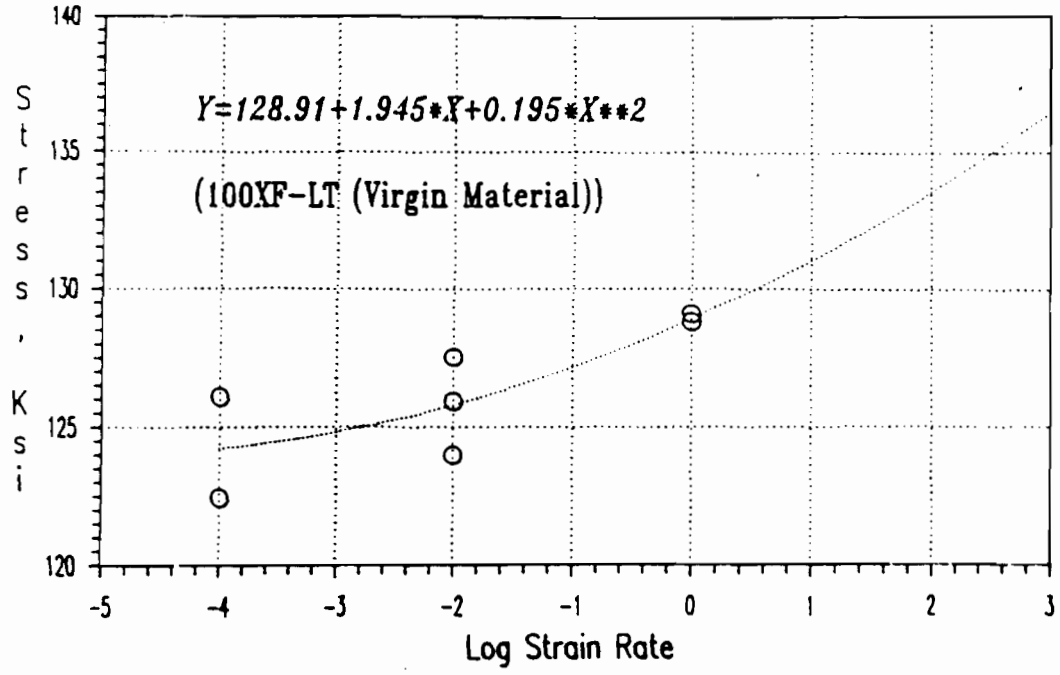

Figure 2.13 Polynomial Equation for Tensile Yield Stress of 100XF-LT Steel (B12)

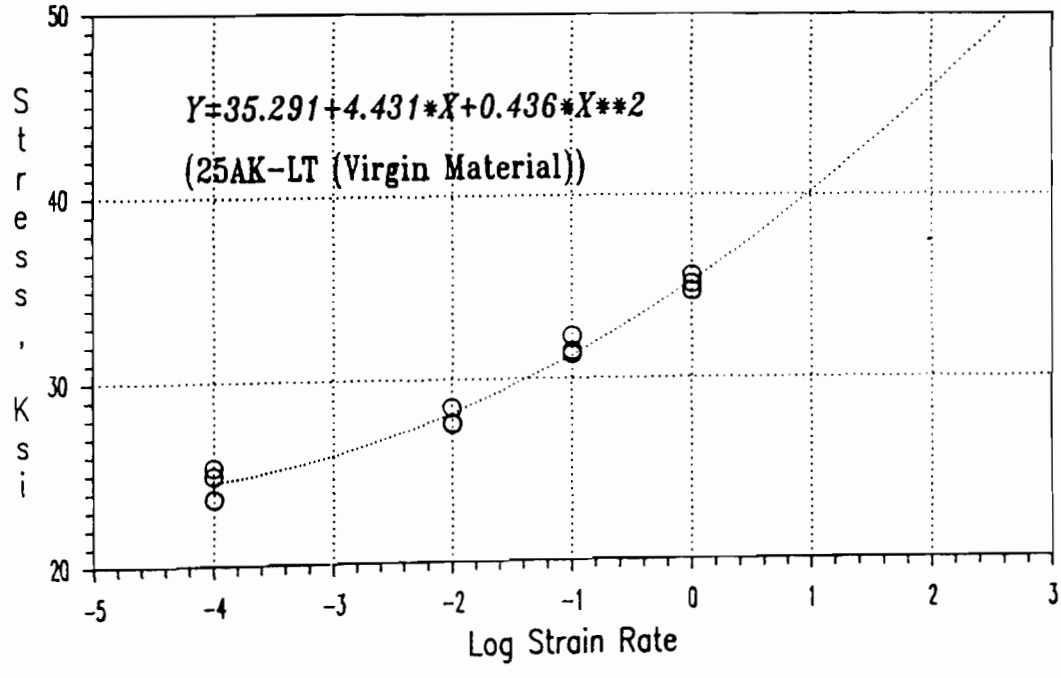

Figure 2.14 Polynomial Equation for Tensile Yield Stress of 25AK-LT Steel (B17)

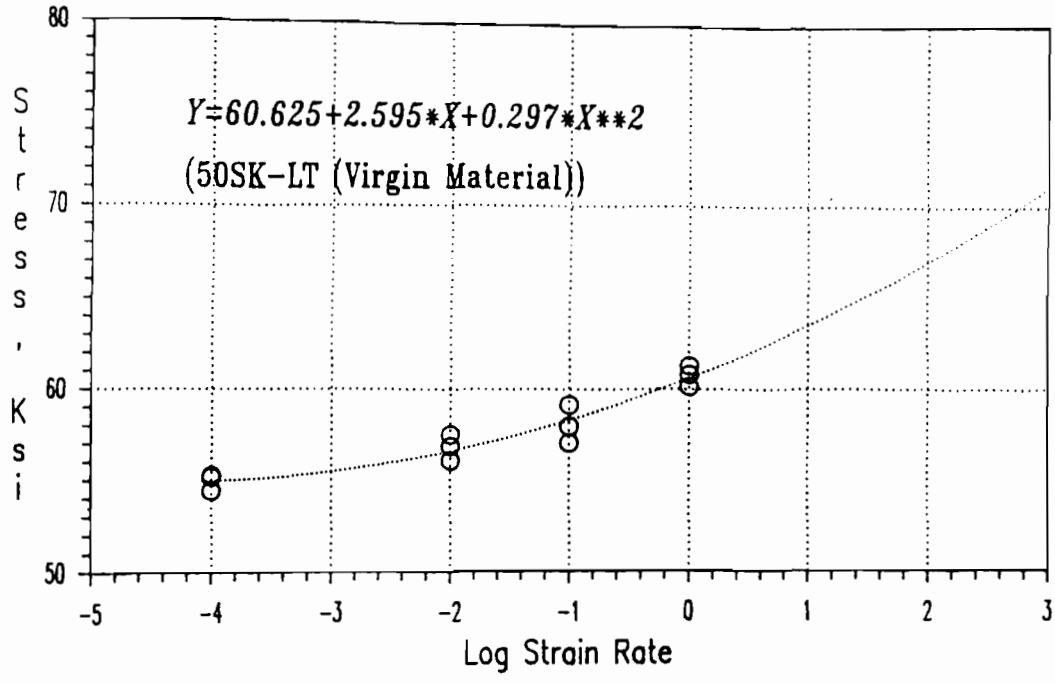

Figure 2.15 Polynomial Equation for Tensile Yield Stress of 50SK-LT Steel (B17)

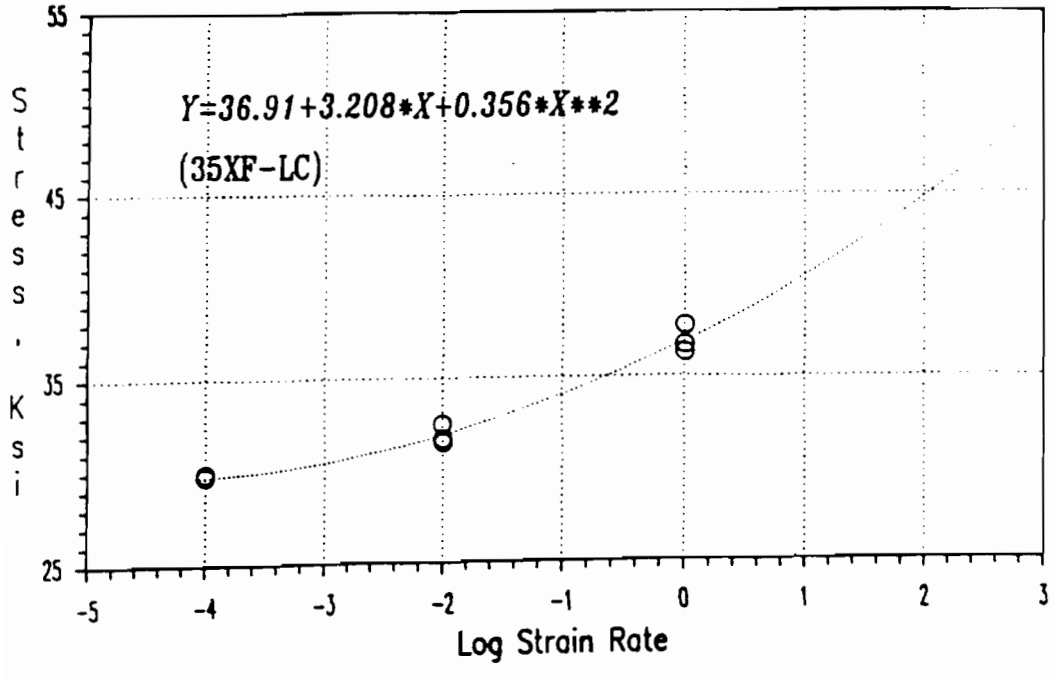

Figure 2.16 Polynomial Equation for Compressive Yield Stress of 35XF-LC Steel (B17)

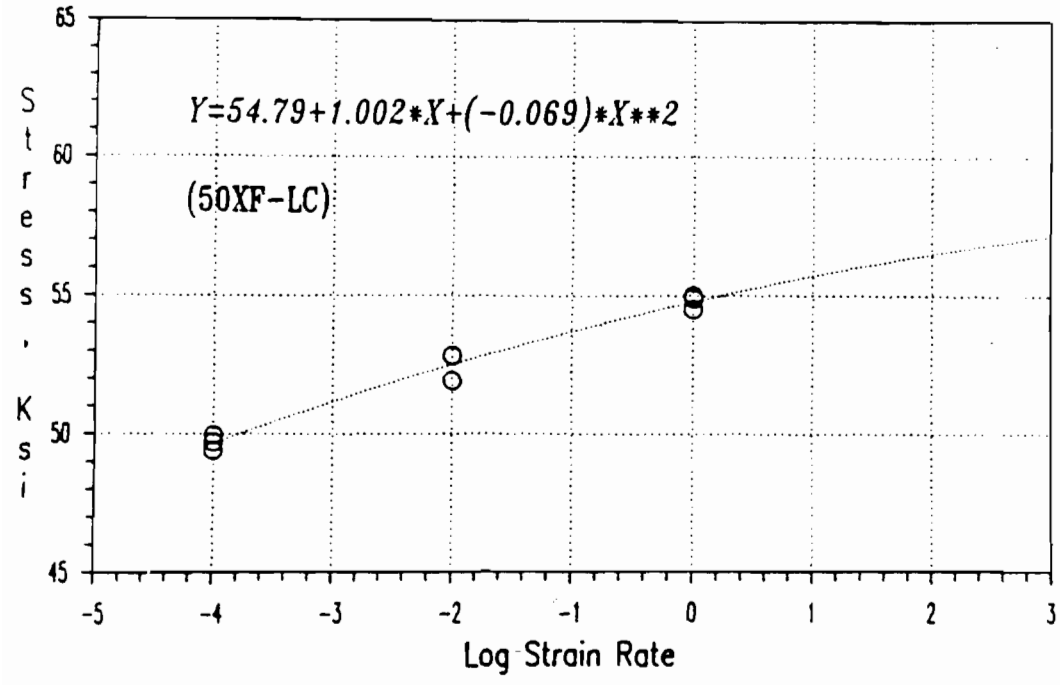

Figure 2.17 Polynomial Equation for Compressive Yield Stress of 50XF-LC Steel (B12)

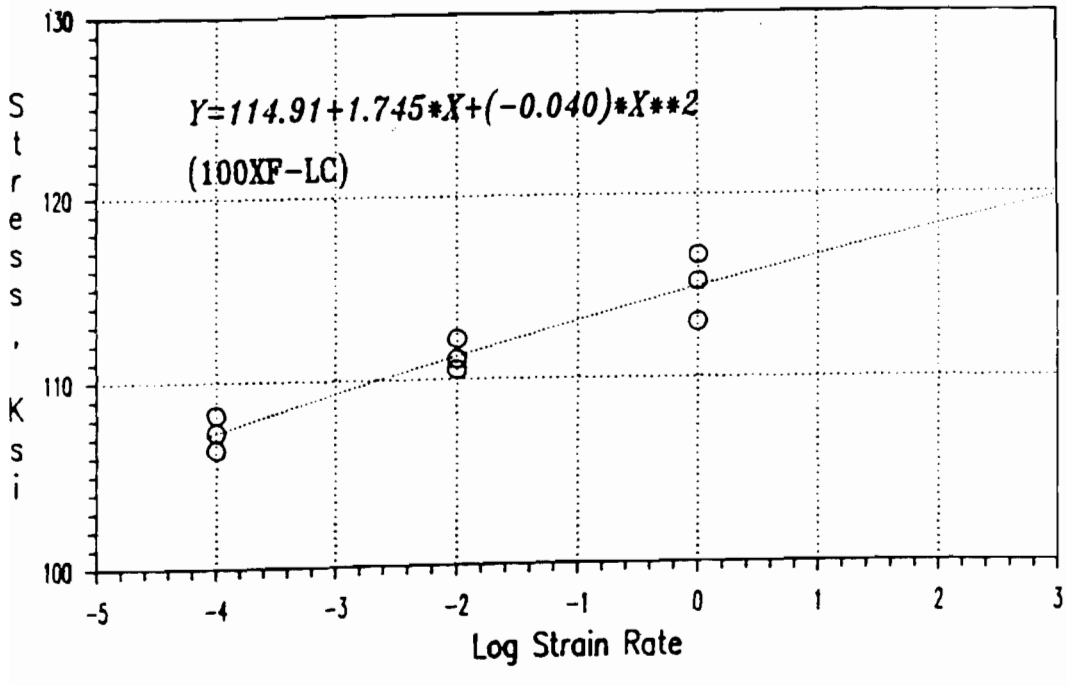

Figure 2.18 Polynomial Equation for Compressive Yield Stress of 100XF-LC Steel (B12)

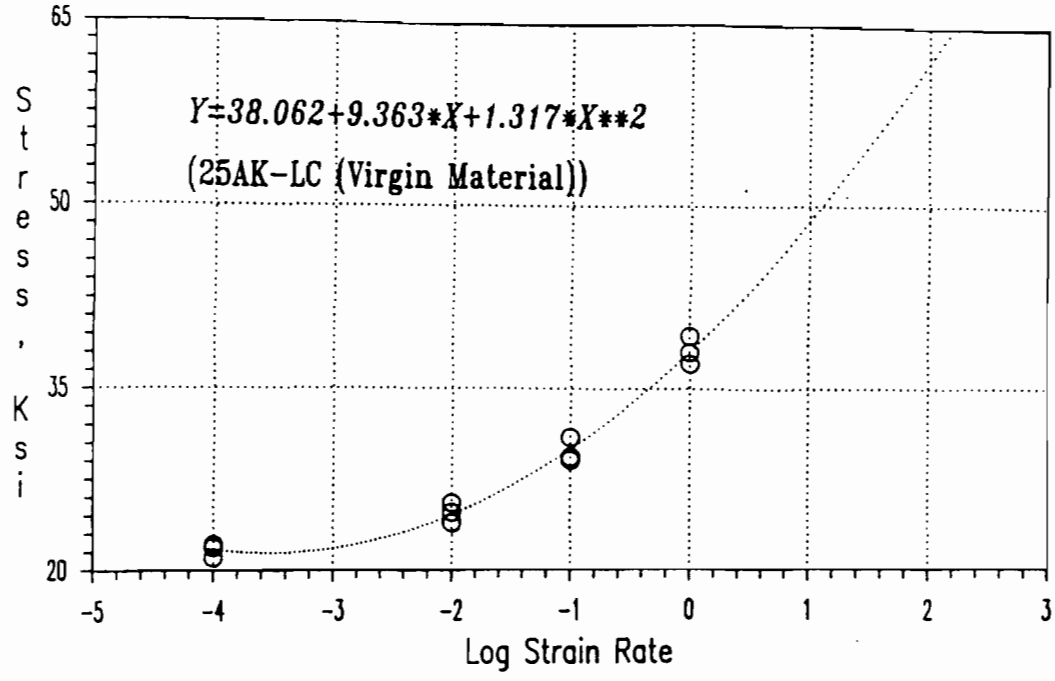

Figure 2.19 Polynomial Equation for Compressive Yield Stress of 25AK-LC Steel (B17)

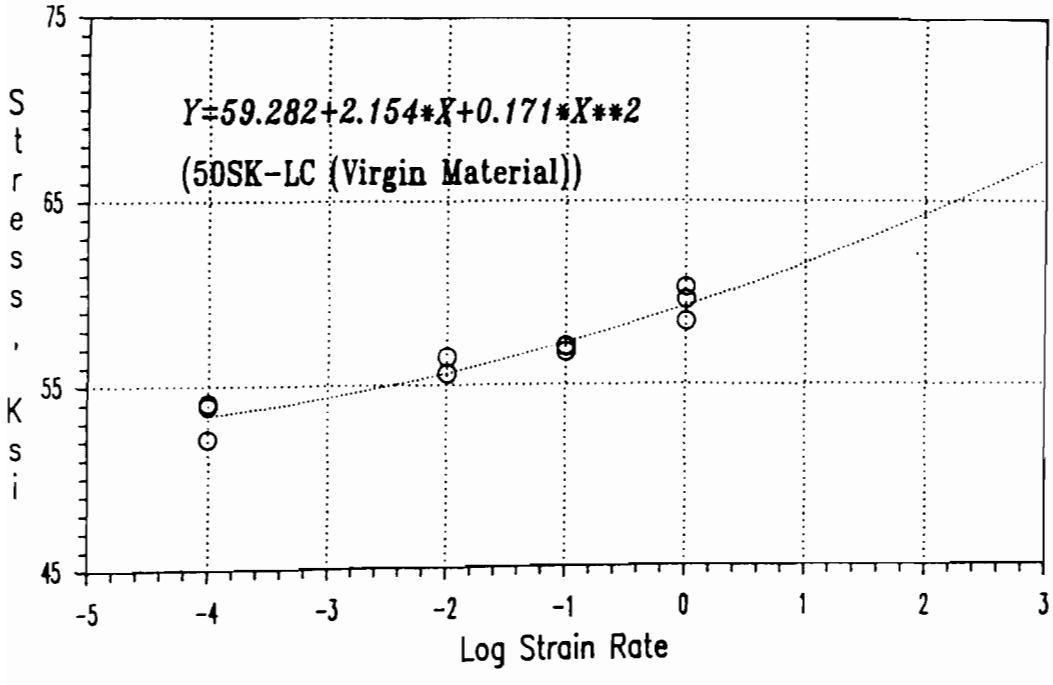

Figure 2.20 Polynomial Equation for Compressive Yield Stress

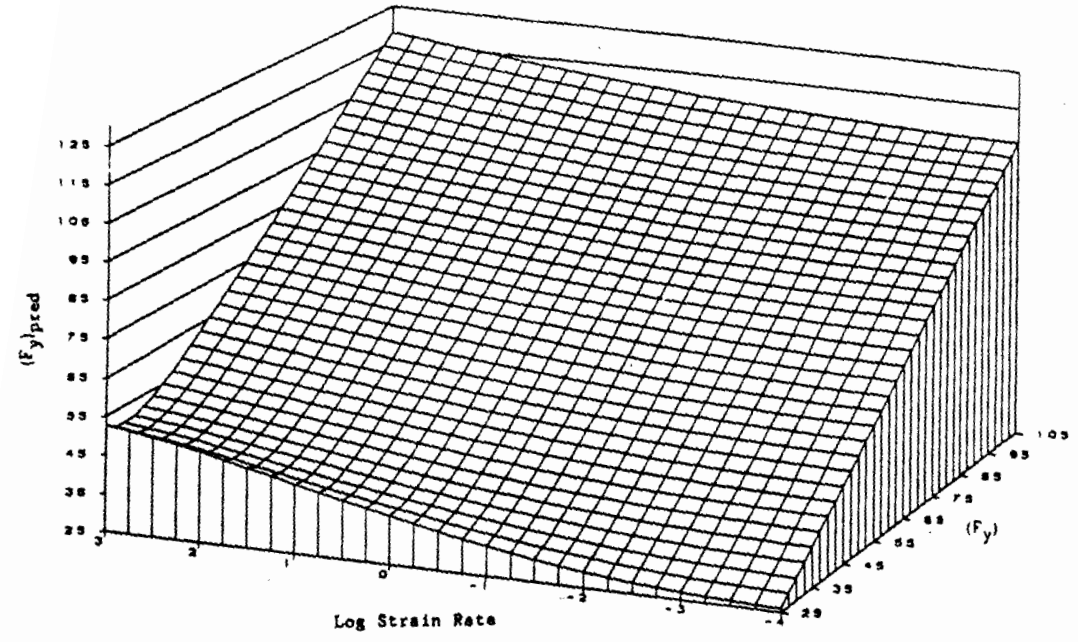

Figure 2.21 Generalized Prediction of Dynamic Tensile Yield Stress (B18)

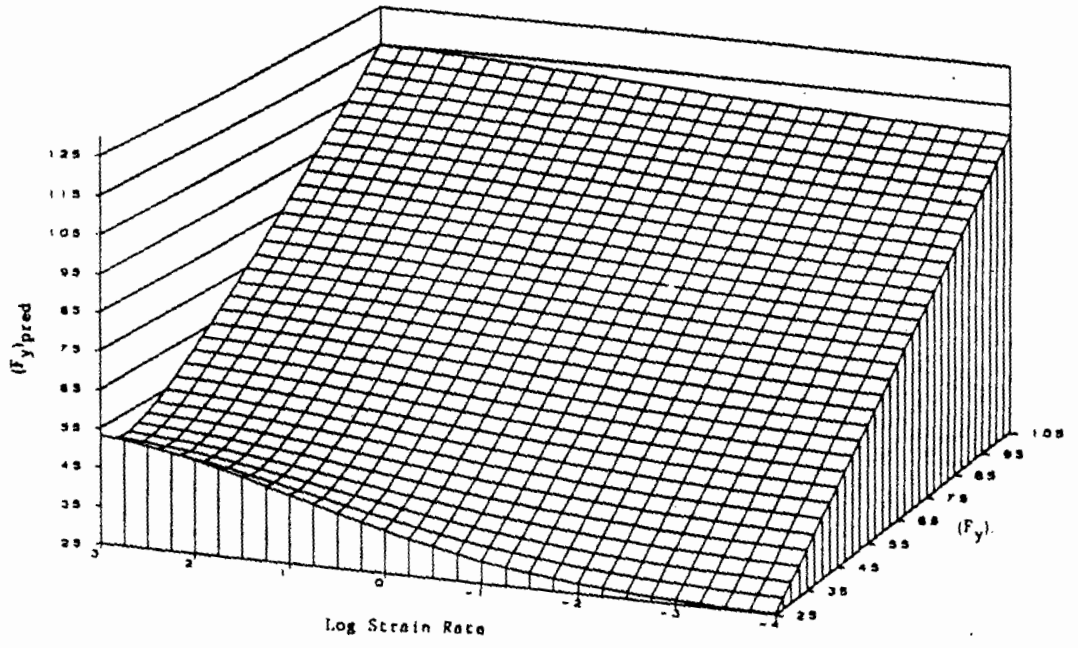

Figure 2.22 Generalized Prediction of Dynamic Compressive Yield Stress (B18)

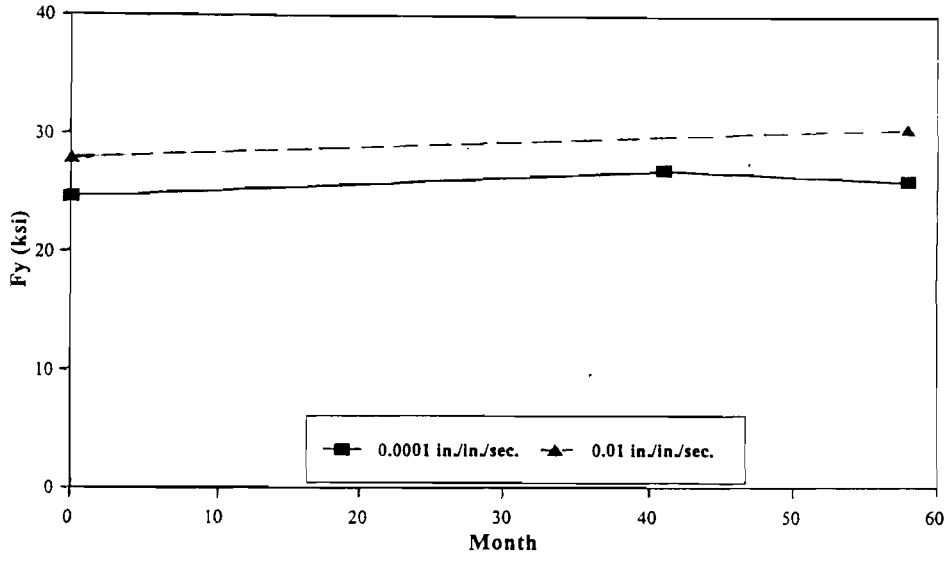

(a) Average Yield Strength vs. Time for 25AK Steel

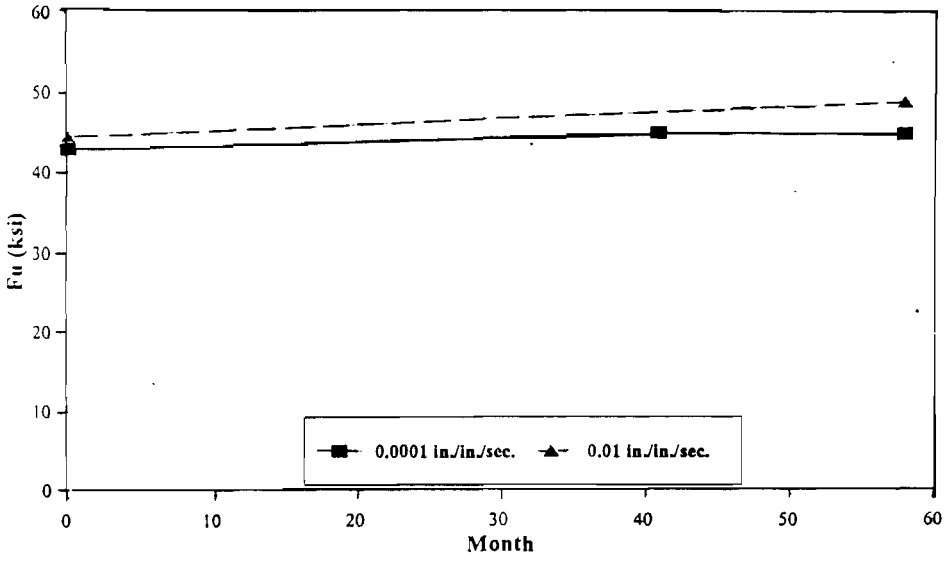

(b) Average Tensile Strength vs. Time for 25AK Steel

Figure 2.23 Aging Effect on the Mechanical Properties of 25AK Sheet Steel (B21)

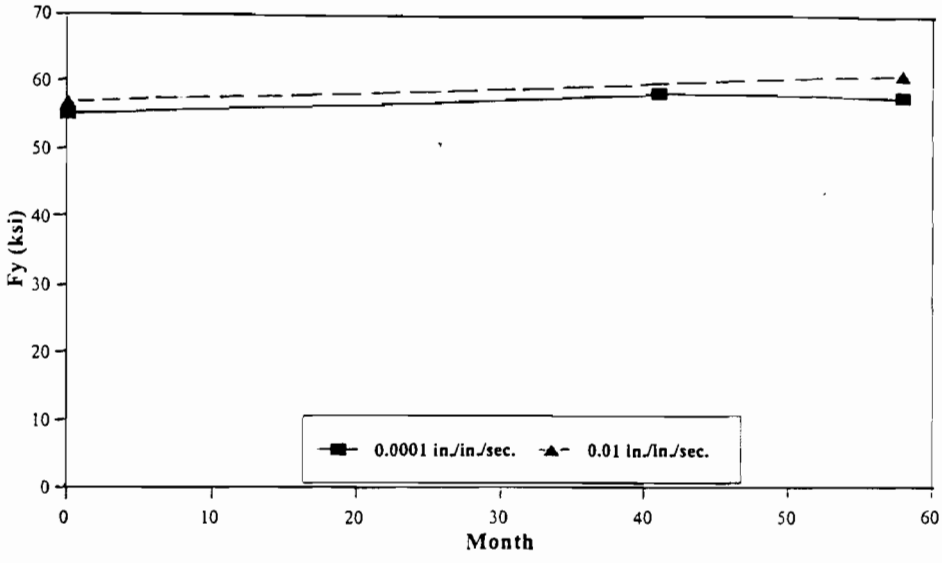

Average Yield Strength vs. Time for 50SK Steel

(a)

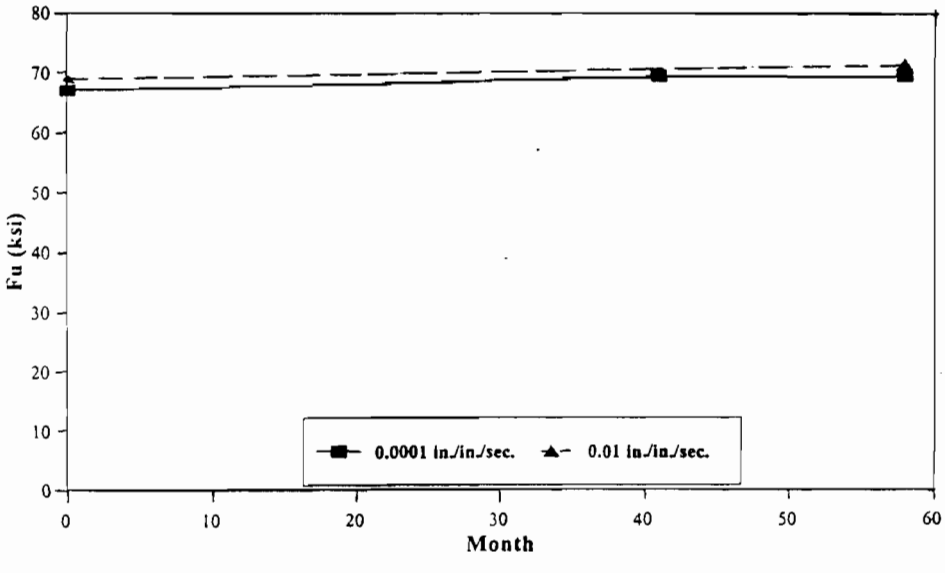

Average Tensile Strength vs. Time for 50SK Steel

(b)

Figure 2.24 Aging Effect on the Mechanical Properties of 50SK Sheet Steel (B21)

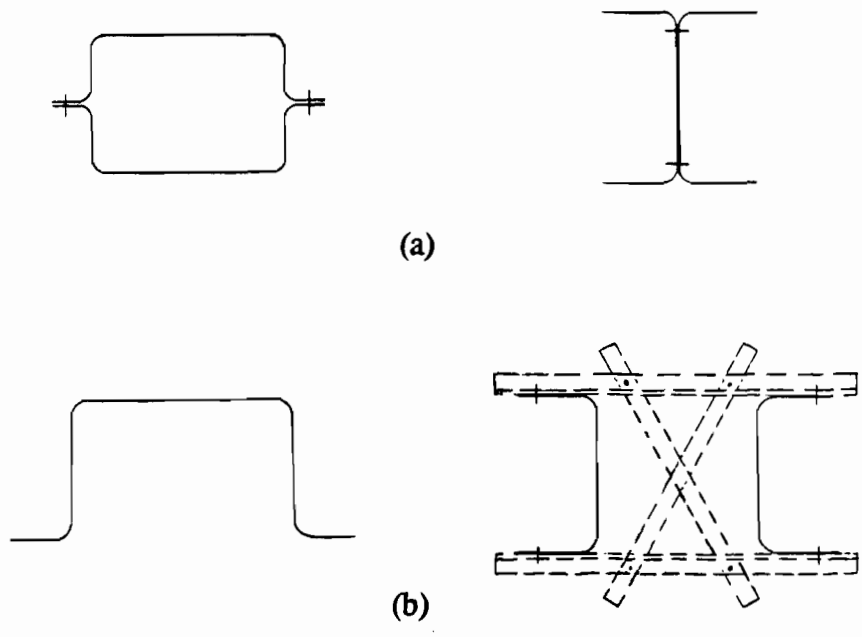

Figure 3.1 Cross Section of Test Specimens.
(a) Stub Columns, (b) Beams (B13)

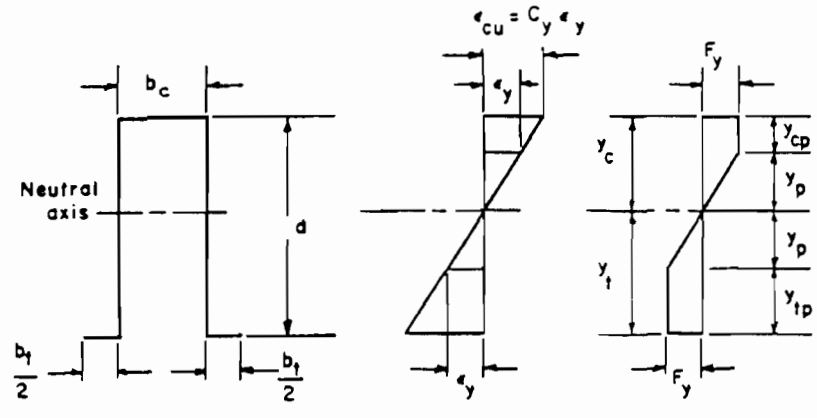

Figure 3.2 Stress Distribution in Sections with Yielded Tension and Compression Flanges at Ultimate Moment (B13)

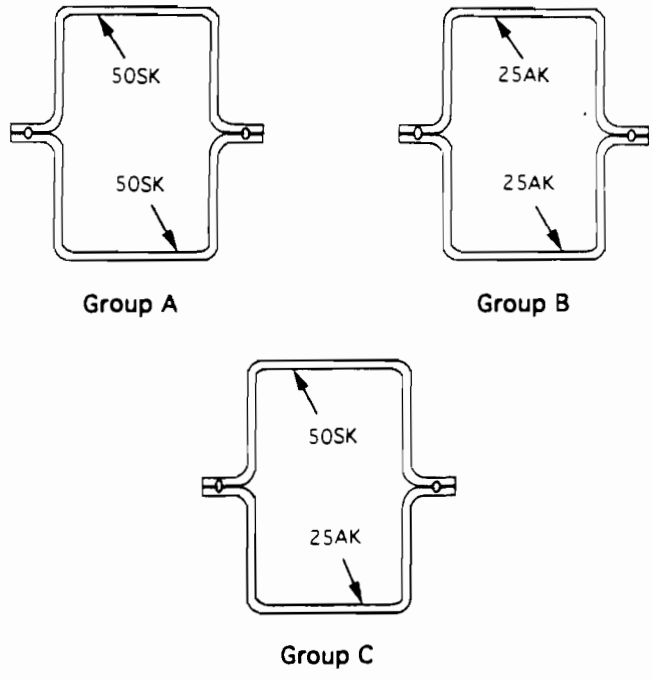

Figure 3.3(a) Cross Section of Box-Shaped Hybrid Stub Columns (B19)

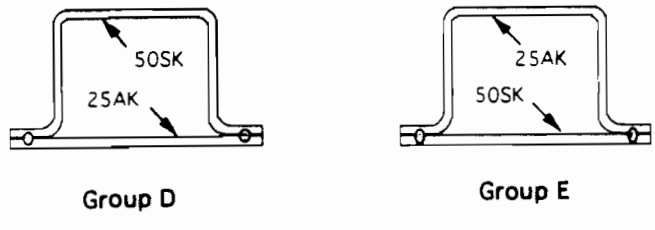

Figure 3.3(b) Cross Section of Hat-Shaped Hybrid Stub Columns (B19)

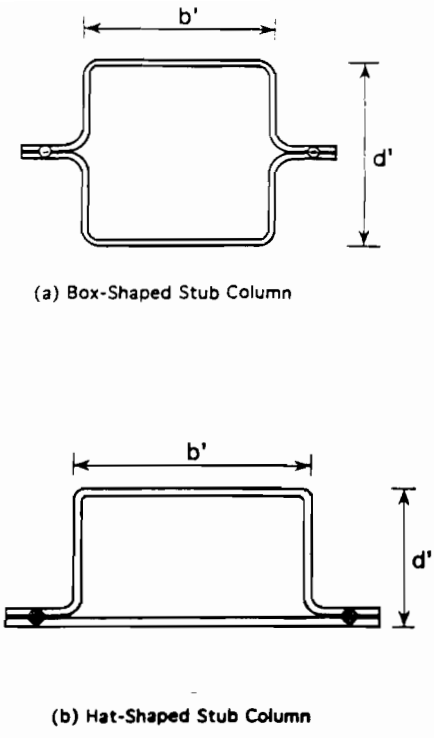

Figure 3.4 Definition of Symbols b' and d' (B19)

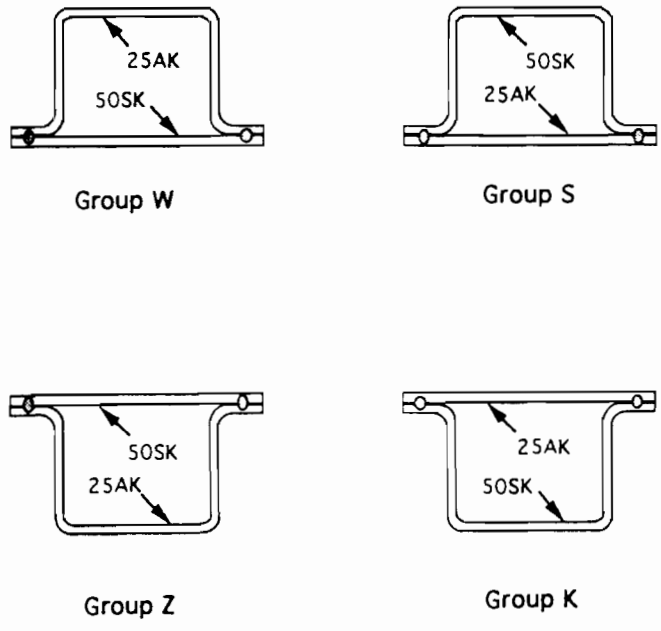

Figure 3.5 Cross Section of Hybrid Beams (B20)

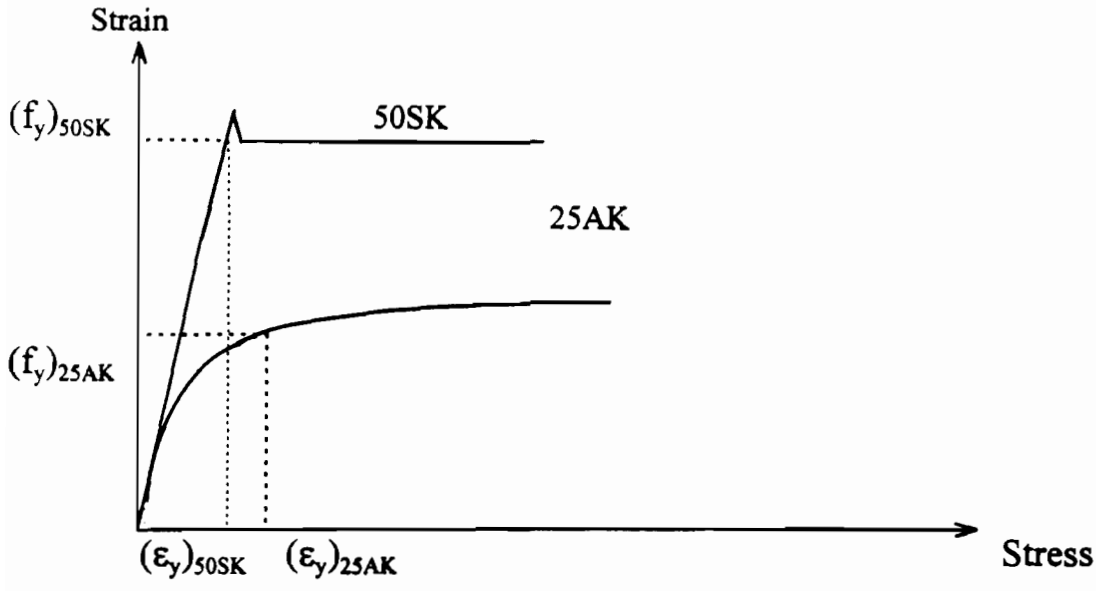

Figure 3.6 **Schematic Sketch of Stress-Strain Relationships for 25AK and 50SK Sheet Steels (B22)**

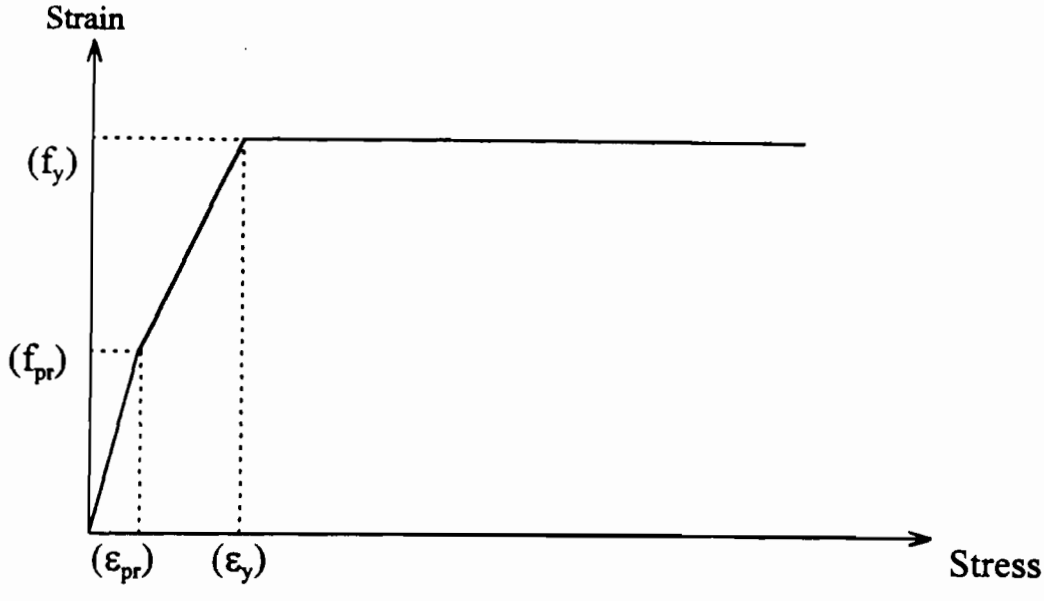

Figure 3.7 **Simulated Stress-Strain Relationships for 25AK and 50SK Sheet Steels (B22)**

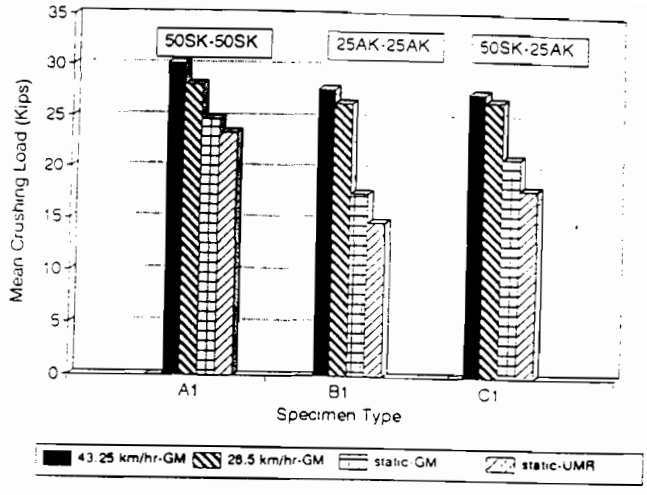

Figure 3.8 **Comparisons of Mean Crushing Loads of Box-Shaped Stub Columns, Small w/t Ratios (B19)**

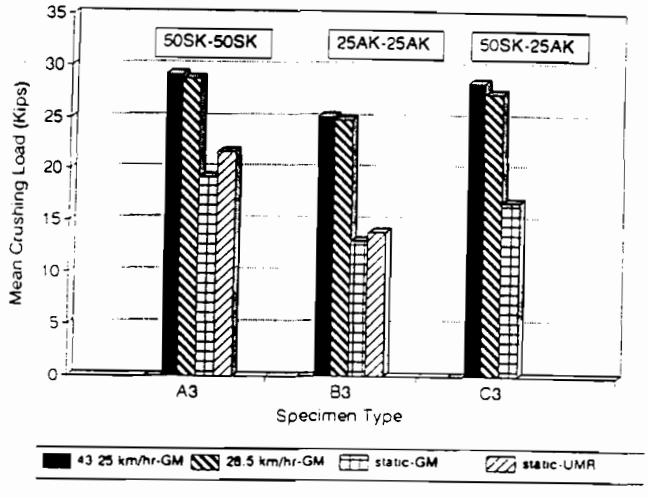

Figure 3.9 **Comparisons of Mean Crushing Loads of Box-Shaped Stub Columns, Large w/t Ratios (B19)**

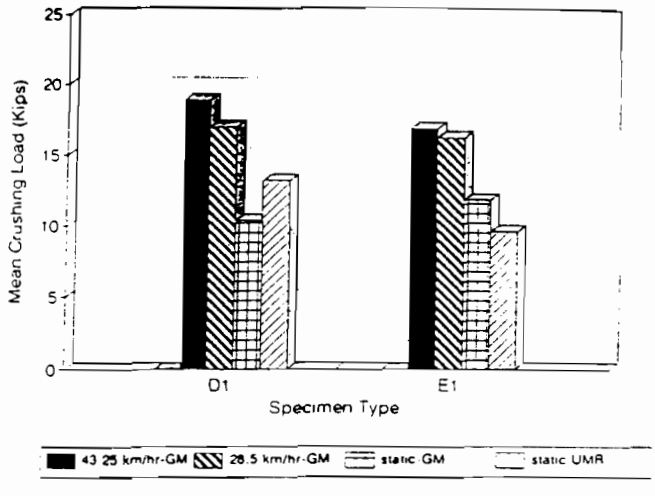

Figure 3.10 **Comparisons of Mean Crushing Loads of Hat-Shaped Stub Columns (B19)**

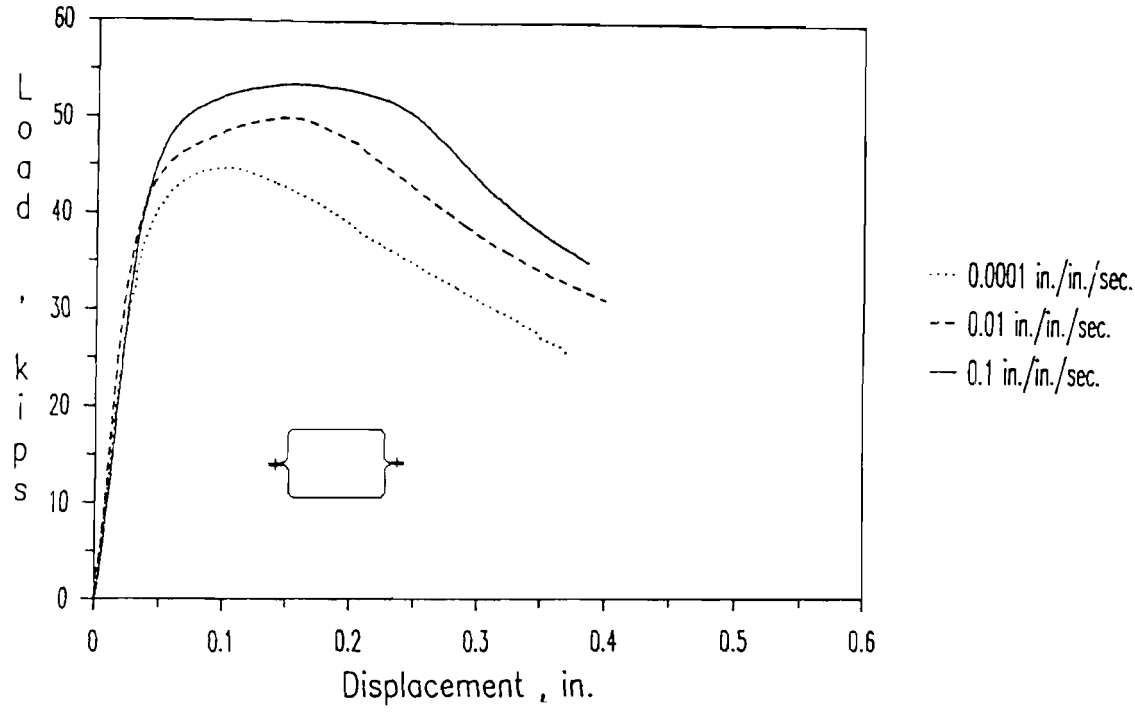

Figure 3.11 Load-Displacement Curves for Stub Columns Using 35XF Sheet Steel (for Stiffened Compression Element, w/t = 27.21) (B18)

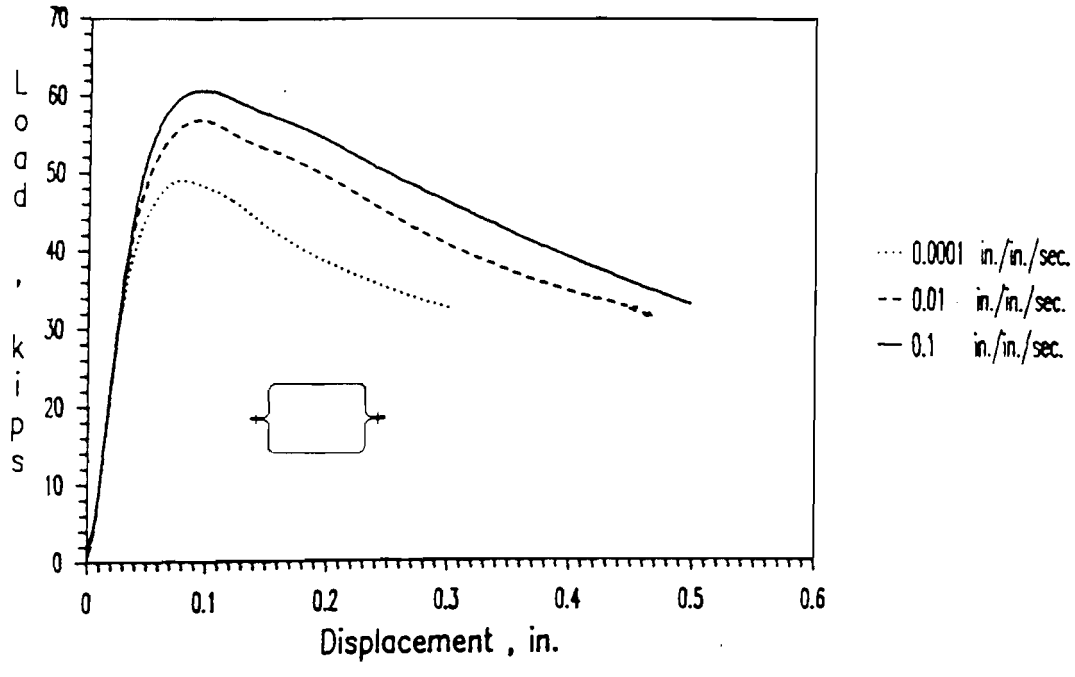

Figure 3.12 Load-Displacement Curves for Stub Columns Using 35XF Sheet Steel (for Stiffened Compression Element, w/t = 38.98) (B18)

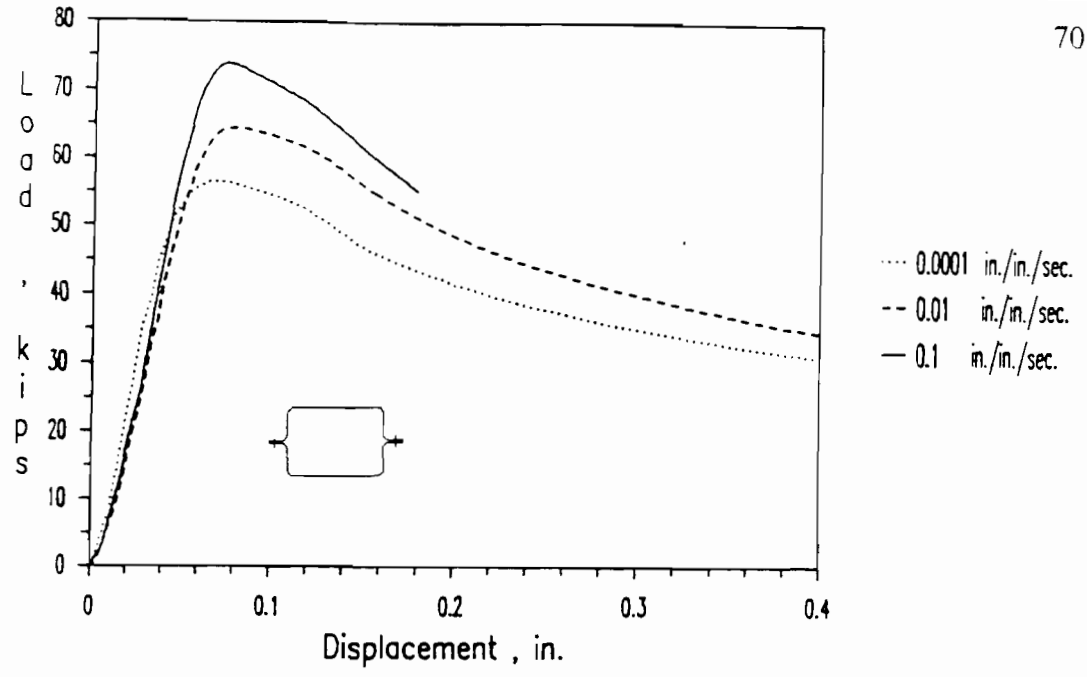

Figure 3.13 Load-Displacement Curves for Stub Columns Using 35XF Sheet Steel (for Stiffened Compression Element, w/t = 52.91) (B18)

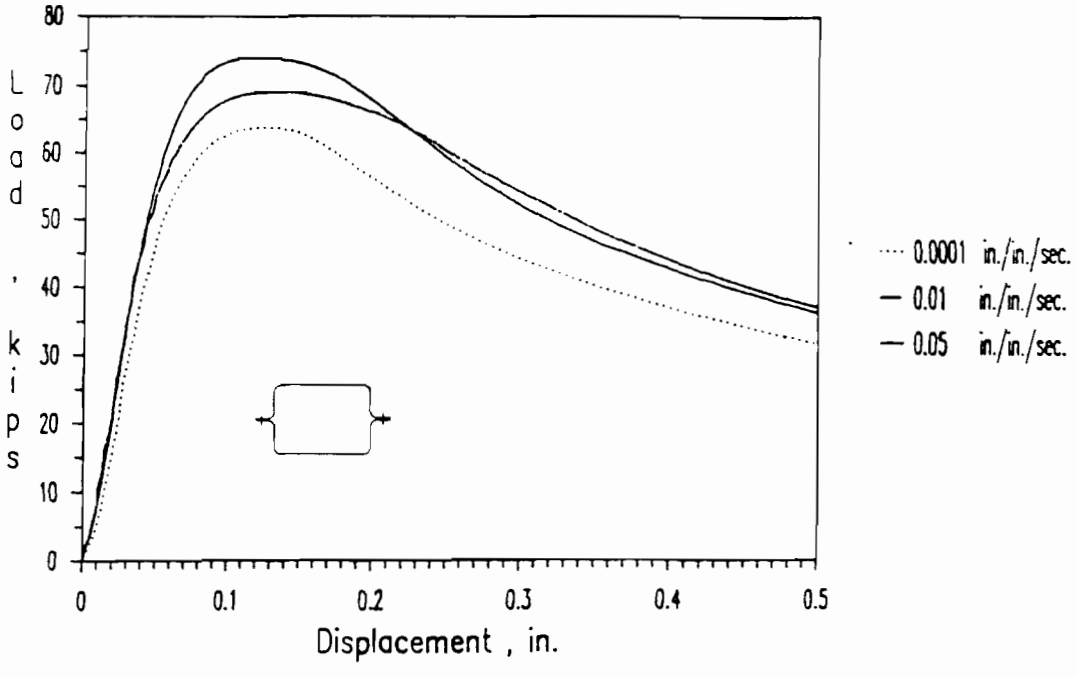

Figure 3.14 Load-Displacement Curves for Stub Columns Using 35XF Sheet Steel (for Stiffened Compression Element, w/t = 100.62) (B18)

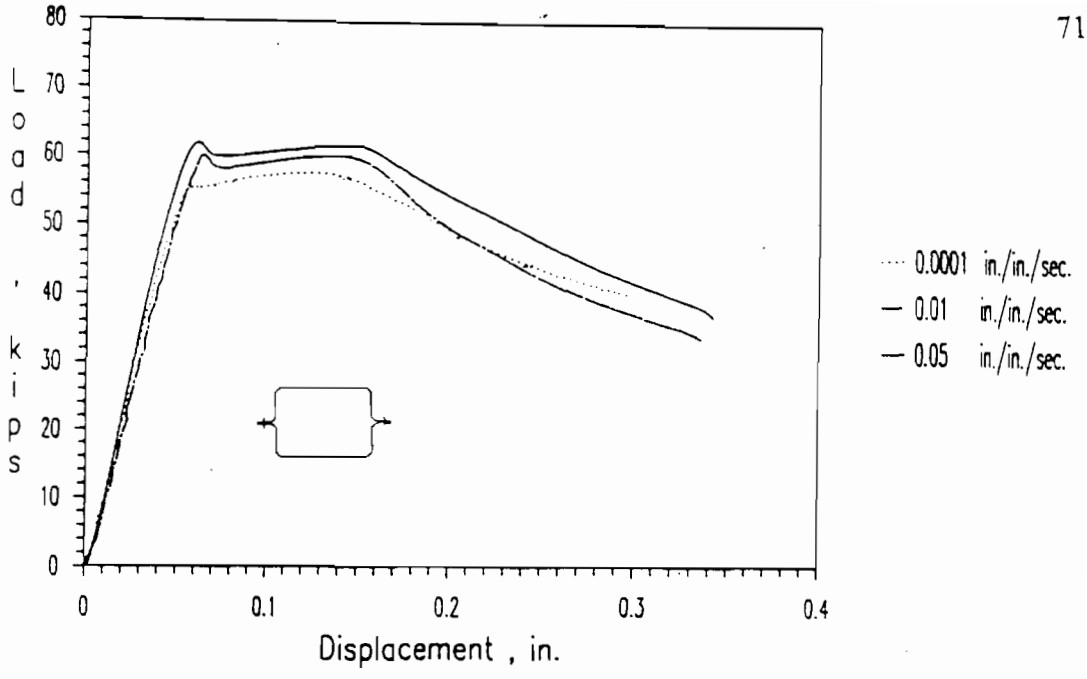

Figure 3.15 Load-Displacement Curves for Stub Columns Using 50XF Sheet Steel (for Stiffened Compression Element, w/t = 23.03) (B18)

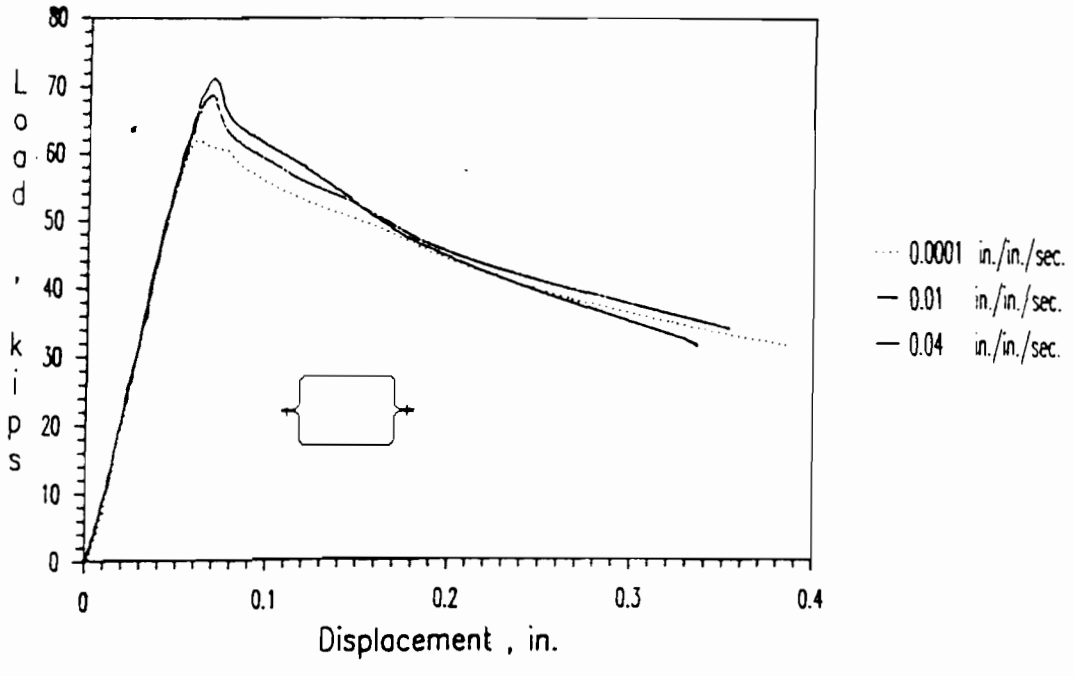

Figure 3.16 Load-Displacement Curves for Stub Columns Using 50XF Sheet Steel (for Stiffened Compression Element, w/t = 34.88) (B18)

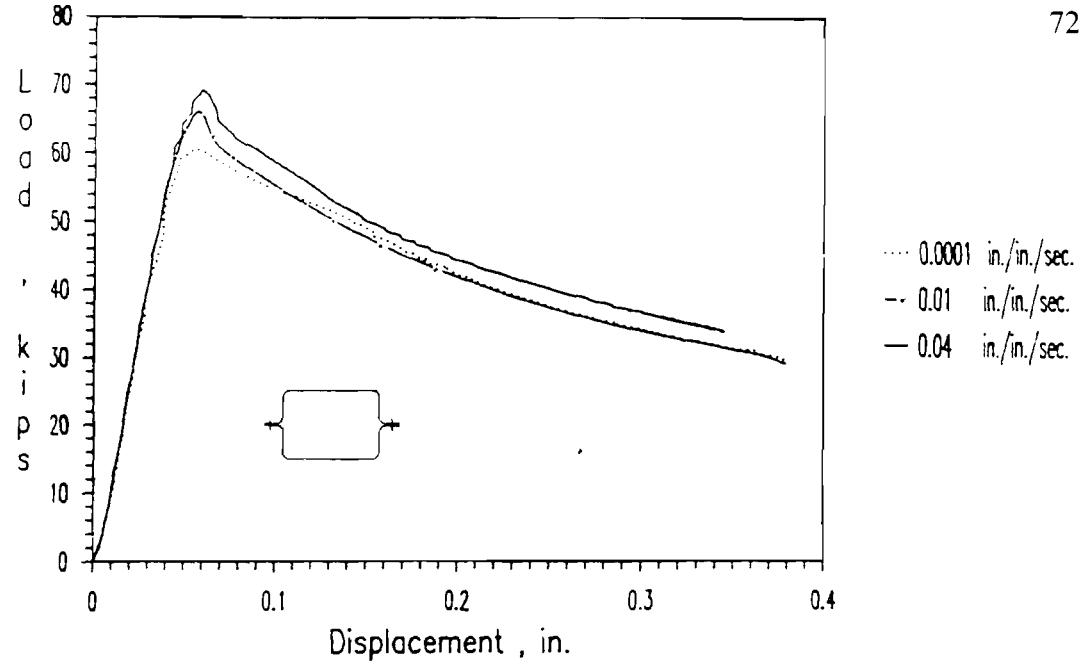

Figure 3.17 Load-Displacement Curves for Stub Columns Using 50XF Sheet Steel (for Stiffened Compression Element, w/t = 52.67) (B18)

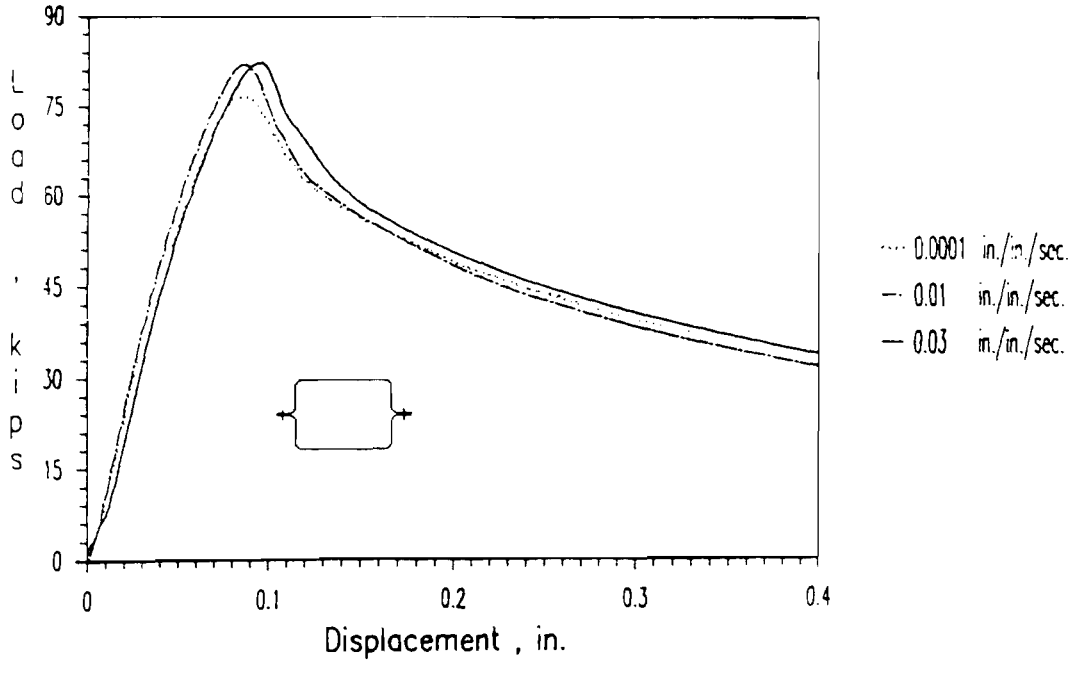

Figure 3.18 Load-Displacement Curves for Stub Columns Using 50XF Sheet Steel (for Stiffened Compression Element, w/t = 98.07) (B18)

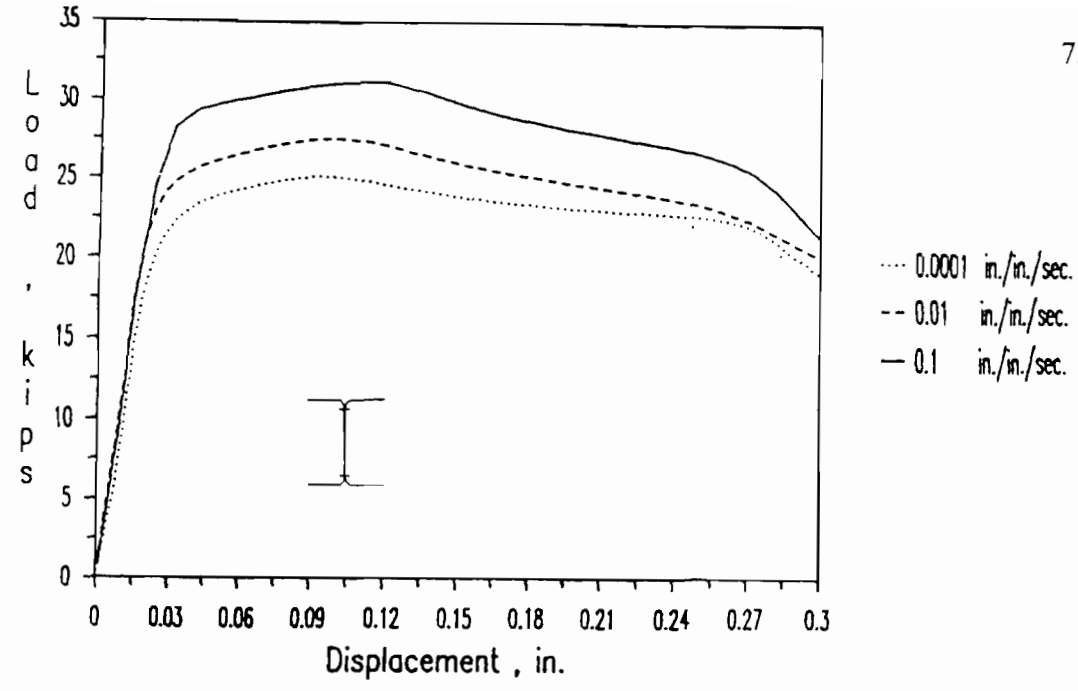

Figure 3.19 Load-Displacement Curves for Stub Columns Using 35XF Sheet Steel (for Unstiffened Compression Element, w/t = 8.98) (B18)

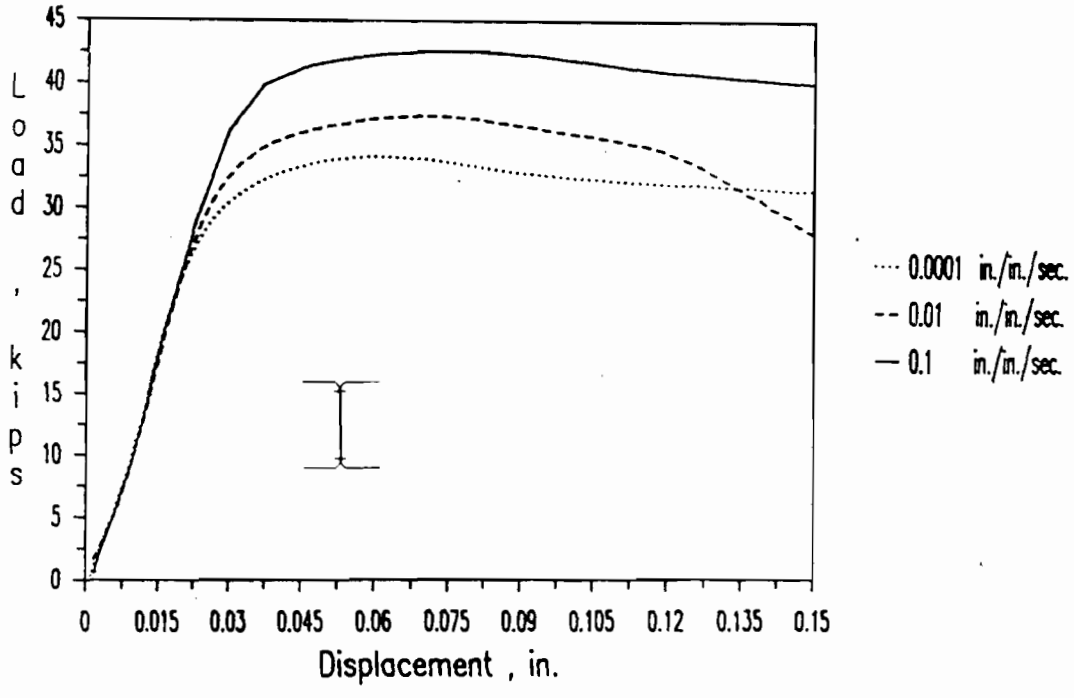

Figure 3.20 Load-Displacement Curves for Stub Columns Using 35XF Sheet Steel (for Unstiffened Compression Element, w/t = 13.38) (B18)

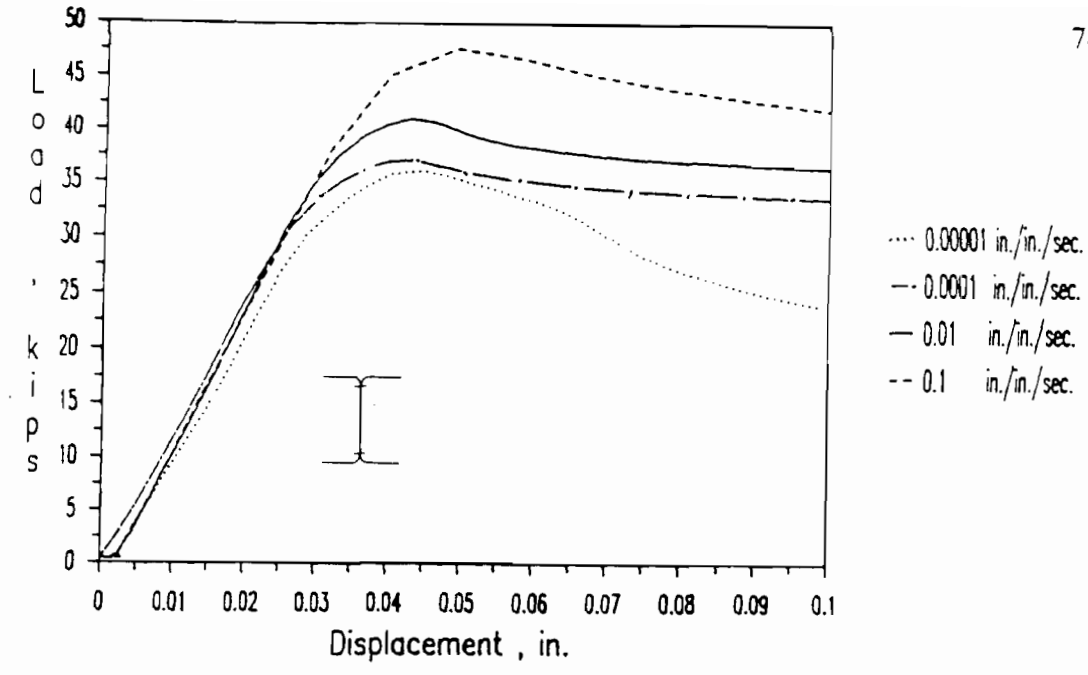

Figure 3.21 Load-Displacement Curves for Stub Columns Using 35XF Sheet Steel (for Unstiffened Compression Element, w/t = 20.87) (B18)

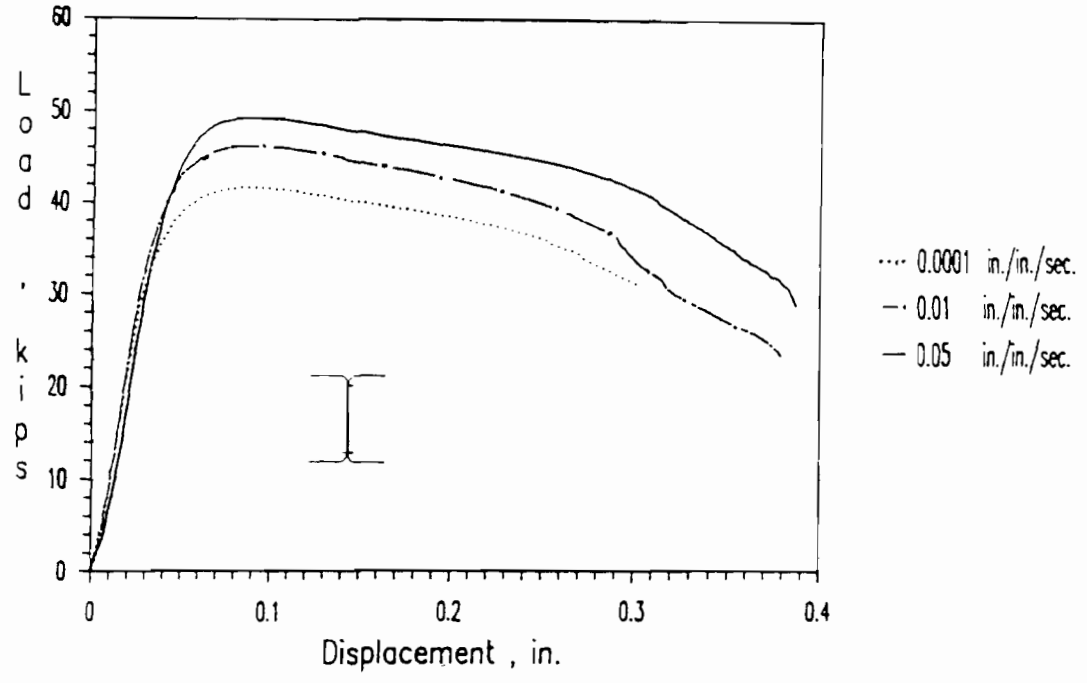

Figure 3.22 Load-Displacement Curves for Stub Columns Using 35XF Sheet Steel (for Unstiffened Compression Element, w/t = 44.57) (B18)

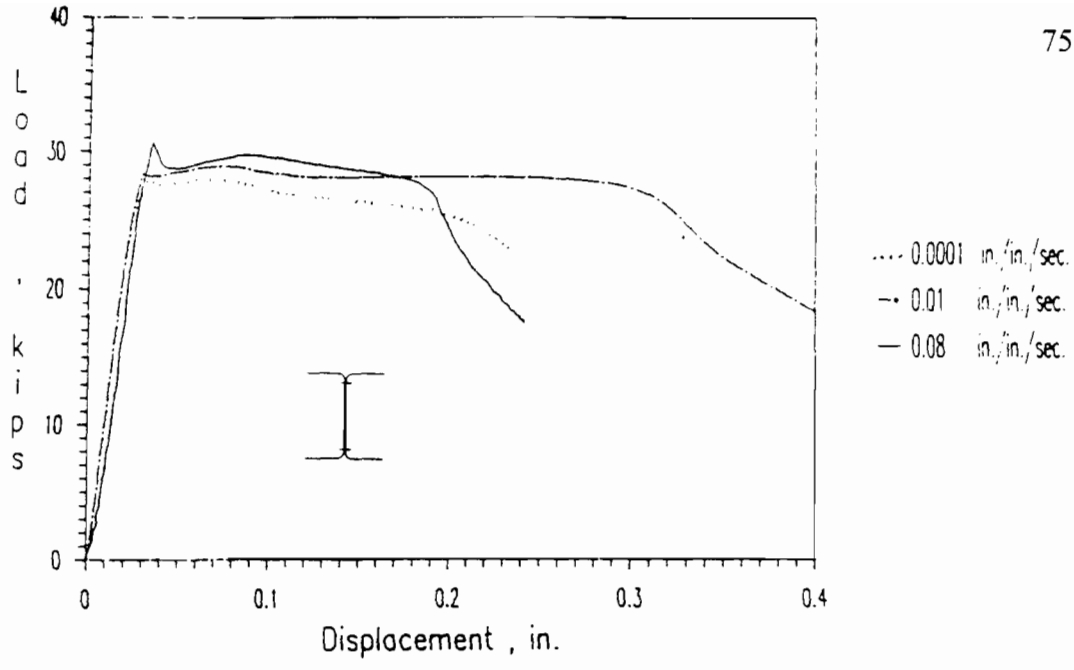

Figure 3.23 Load-Displacement Curves for Stub Columns Using 50XF Sheet Steel (for Unstiffened Compression Element, w/t = 8.37) (B18)

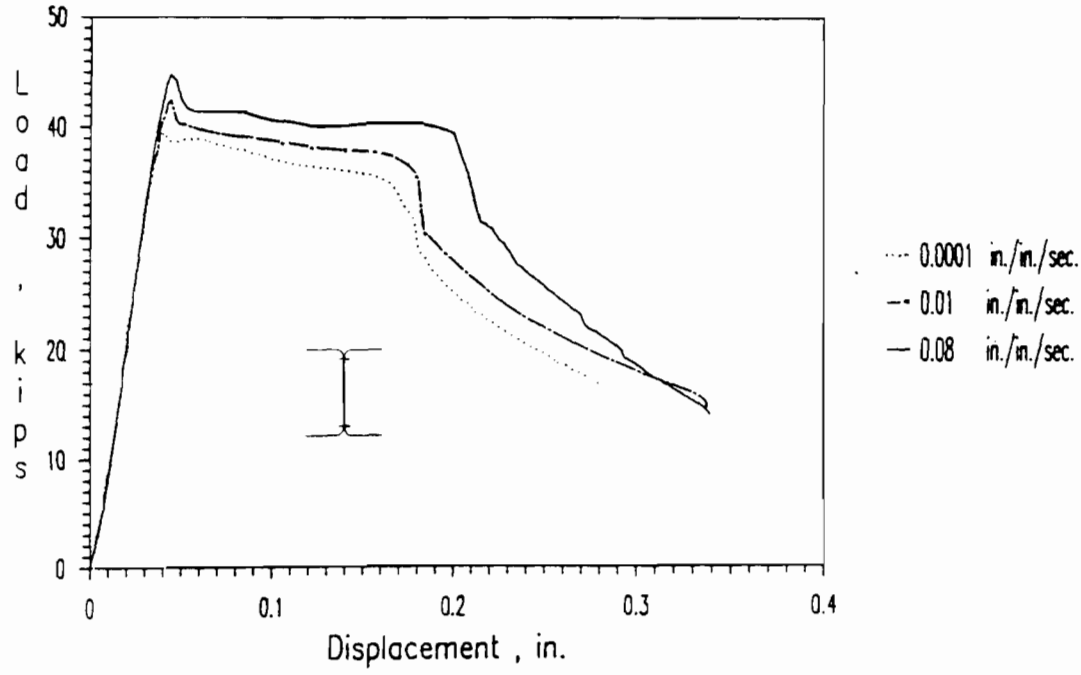

Figure 3.24 Load-Displacement Curves for Stub Columns Using 50XF Sheet Steel (for Unstiffened Compression Element, w/t = 11.59) (B18)

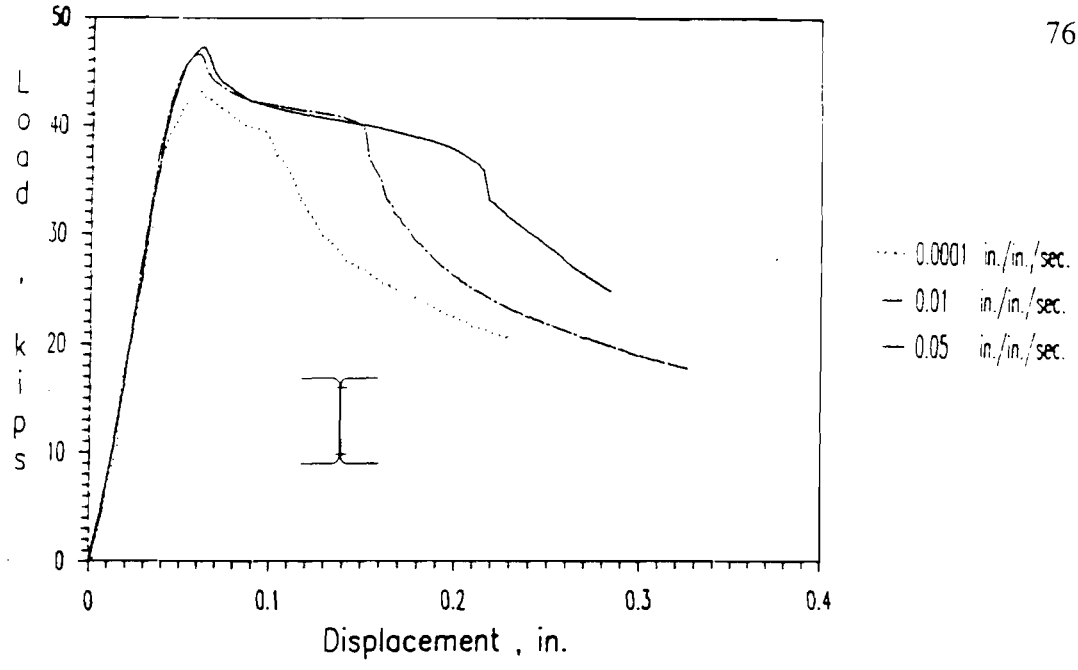

Figure 3.25 Load-Displacement Curves for Stub Columns Using 50XF Sheet Steel (for Unstiffened Compression Element, w/t = 22.77) (B18)

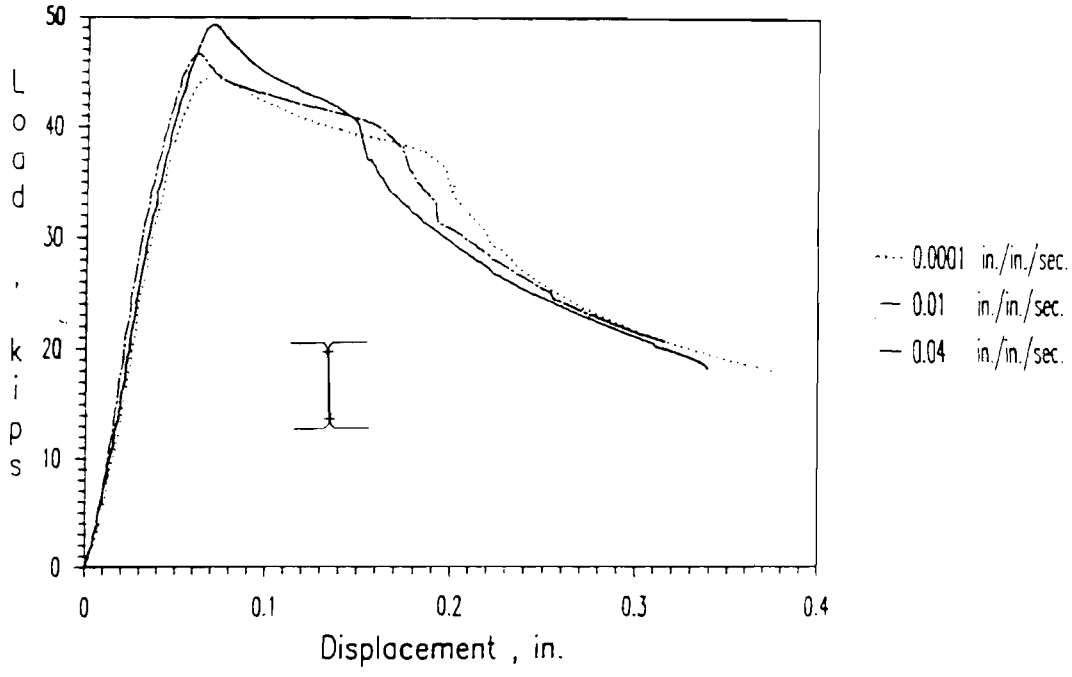

Figure 3.26 Load-Displacement Curves for Stub Columns Using 50XF Sheet Steel (for Unstiffened Compression Element, w/t = 35.27) (B18)

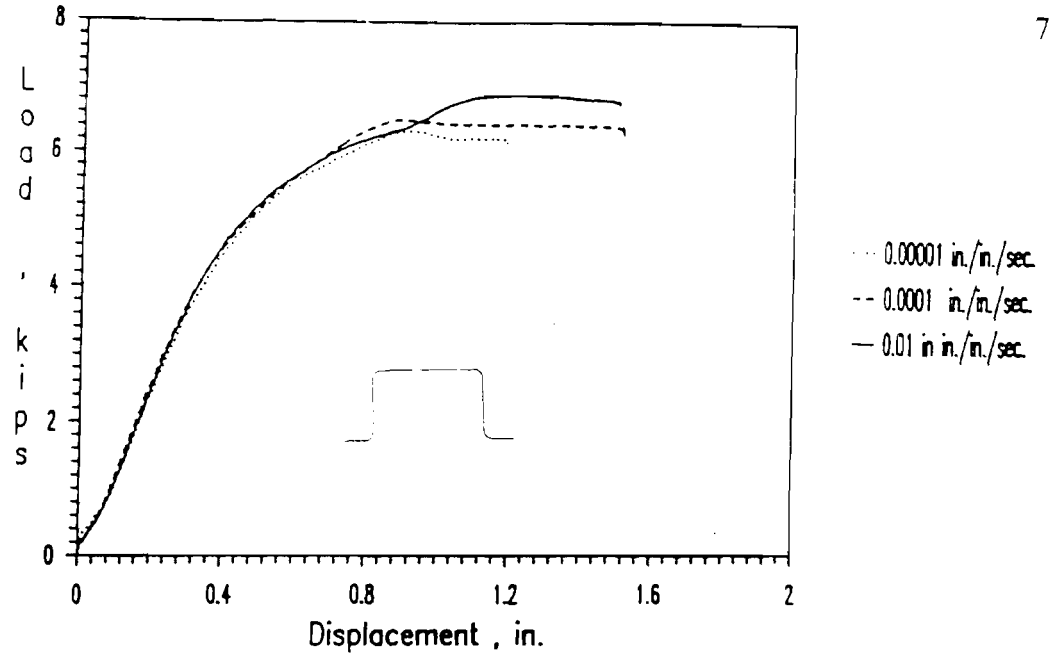

Figure 3.27 Load-Displacement Curves for Hat-Shaped Beams Using 35XF Sheet Steel (for Stiffened Compression Element, w/t = 55.74) (B18)

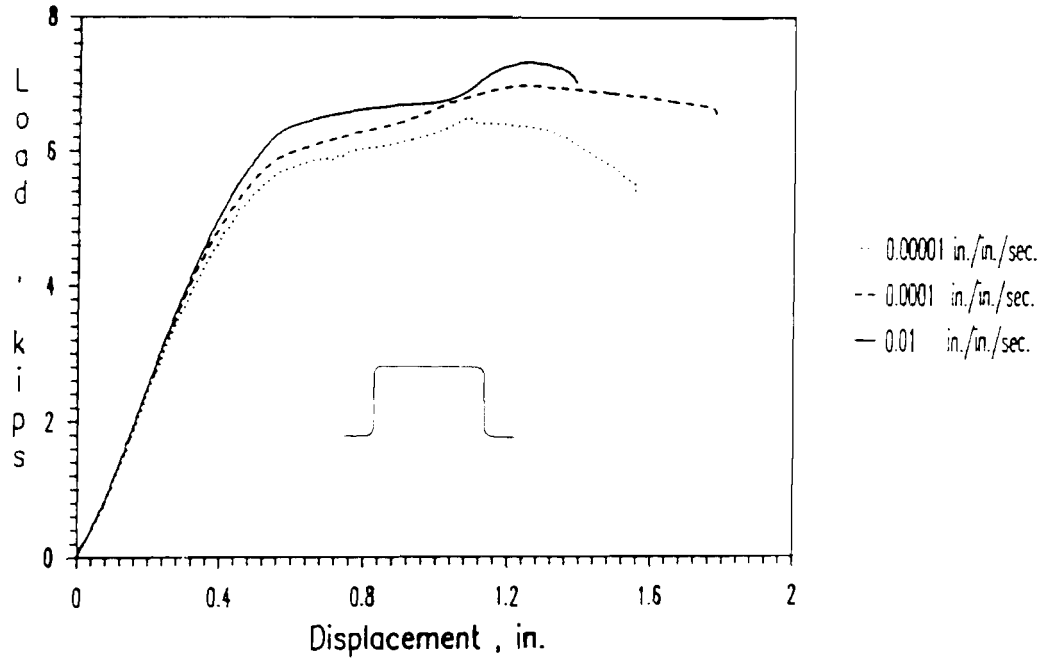

Figure 3.28 Load-Displacement Curves for Hat-Shaped Beams Using 35XF Sheet Steel (for Stiffened Compression Element, w/t = 76.41) (B18)

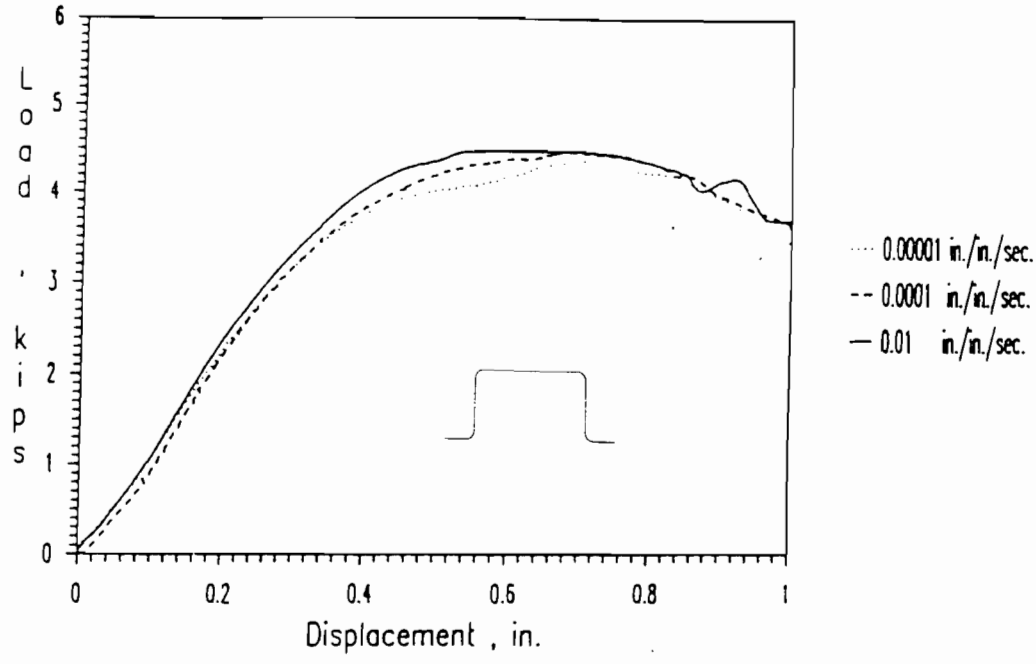

Figure 3.29 Load-Displacement Curves for Hat-Shaped Beams Using 50XF Sheet Steel (for Stiffened Compression Element, w/t = 26.68) (B18)

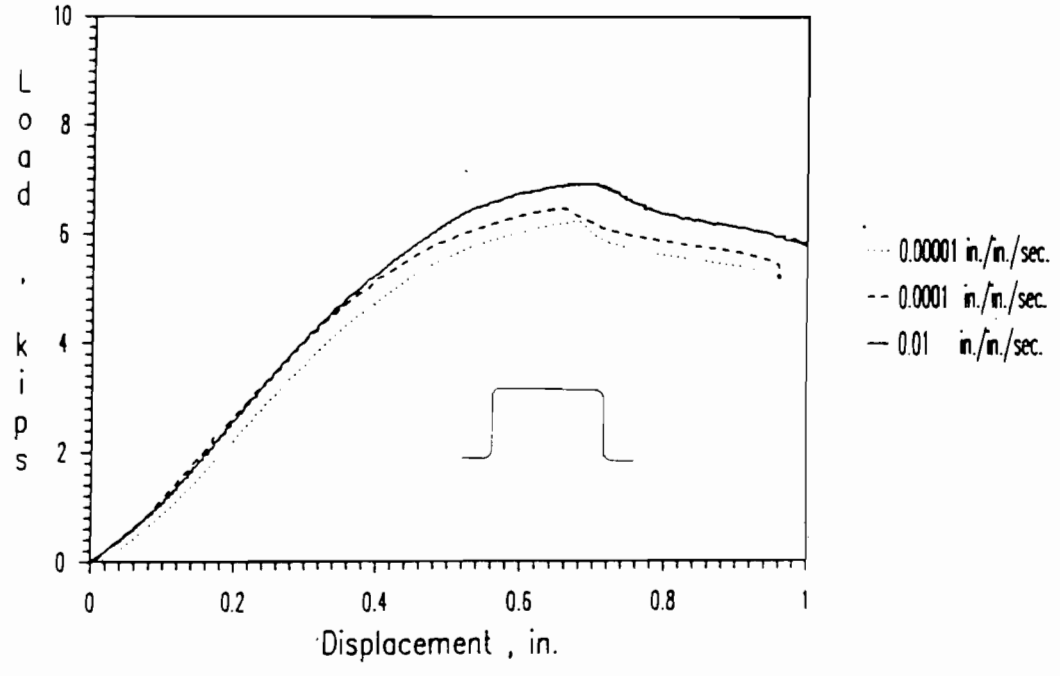

Figure 3.30 Load-Displacement Curves for Hat-Shaped Beams Using 50XF Sheet Steel (for Stiffened Compression Element, w/t = 46.09) (B18)

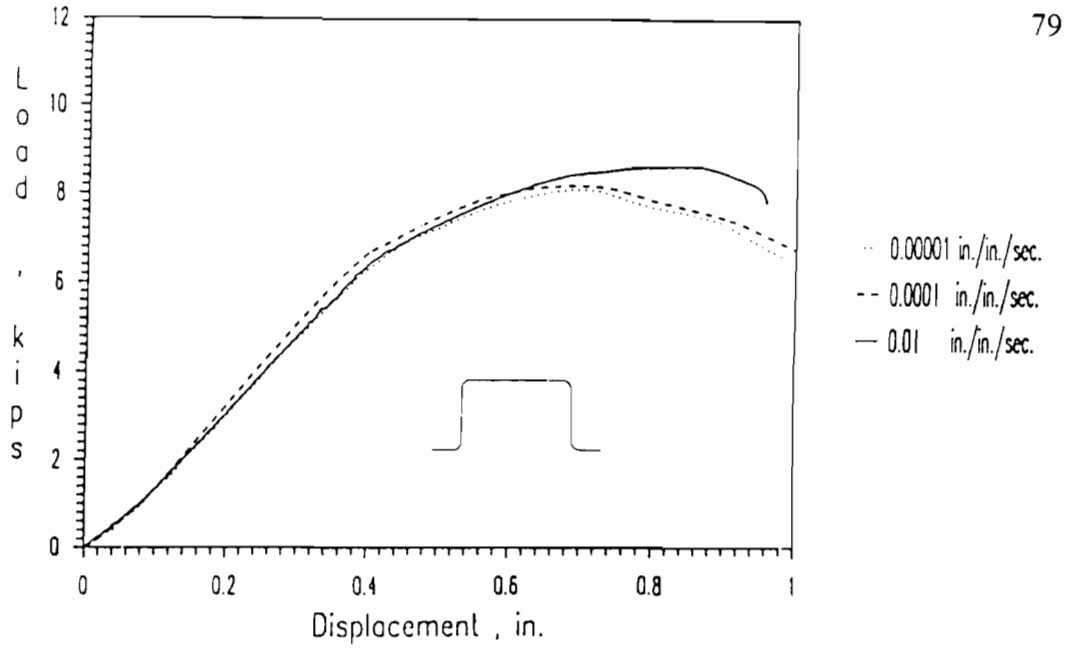

Figure 3.31 Load-Displacement Curves for Hat-Shaped Beams Using 50XF Sheet Steel (for Stiffened Compression Element, w/t = 65.77) (B18)

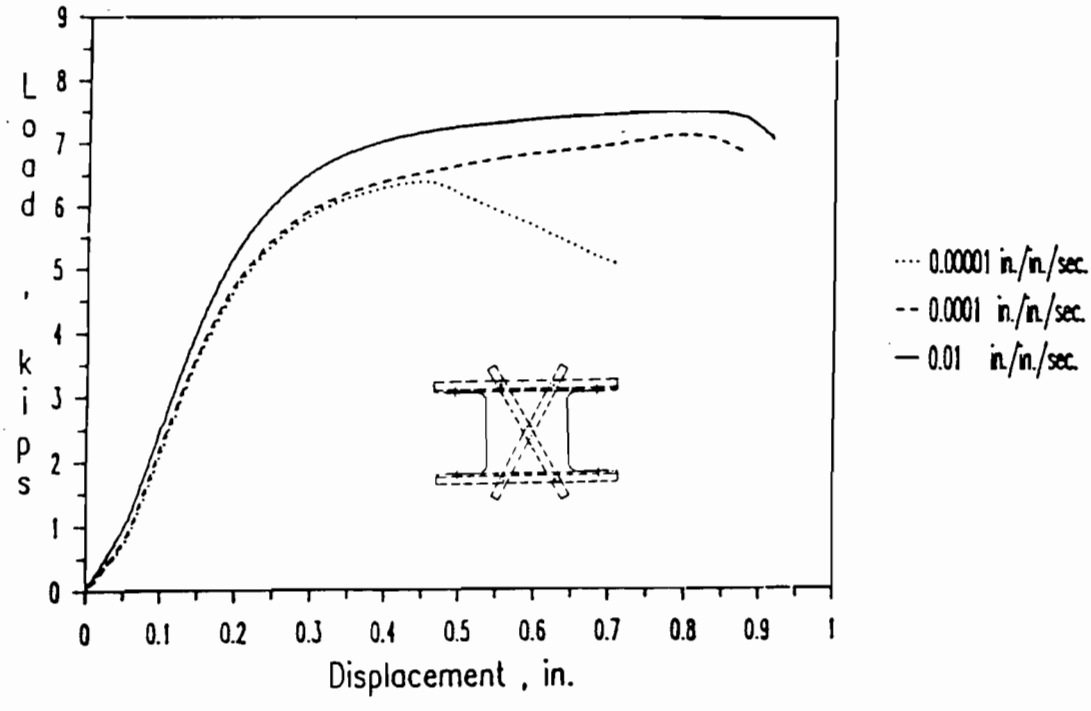

Figure 3.32 Load-Displacement Curves for Channel Beams Using 35XF Sheet Steel (for Unstiffened Compression Element, w/t = 9.17) (B18)

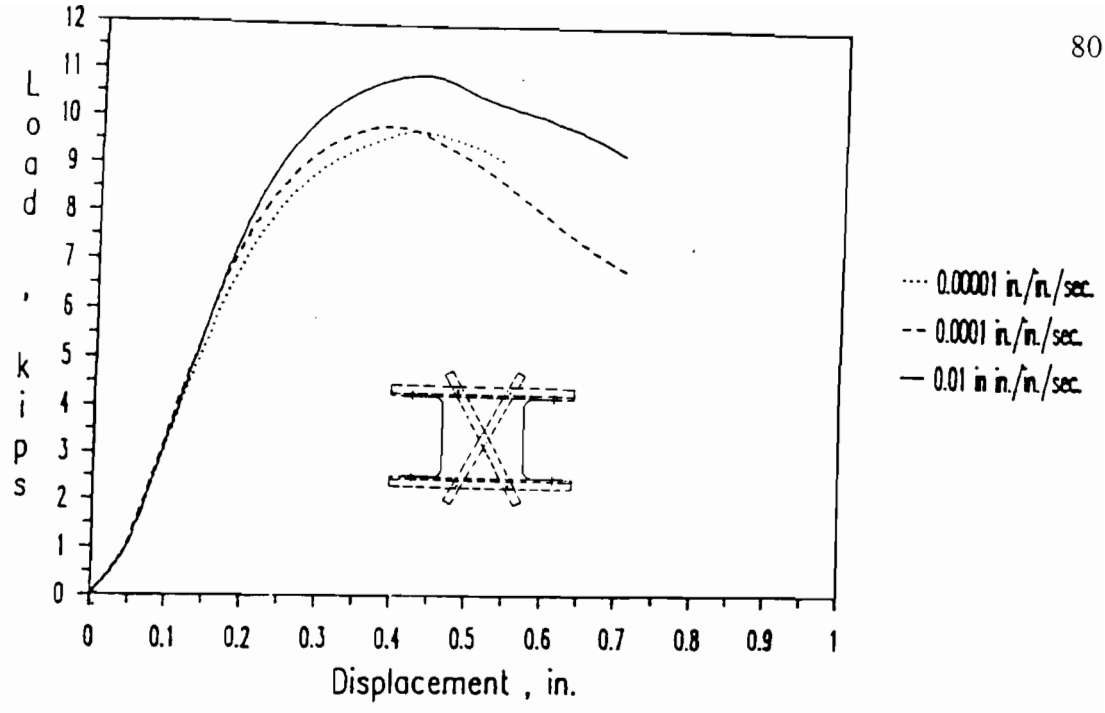

Figure 3.33 Load-Displacement Curves for Channel Beams Using 35XF Sheet Steel (for Unstiffened Compression Element, w/t = 15.08) (B18)

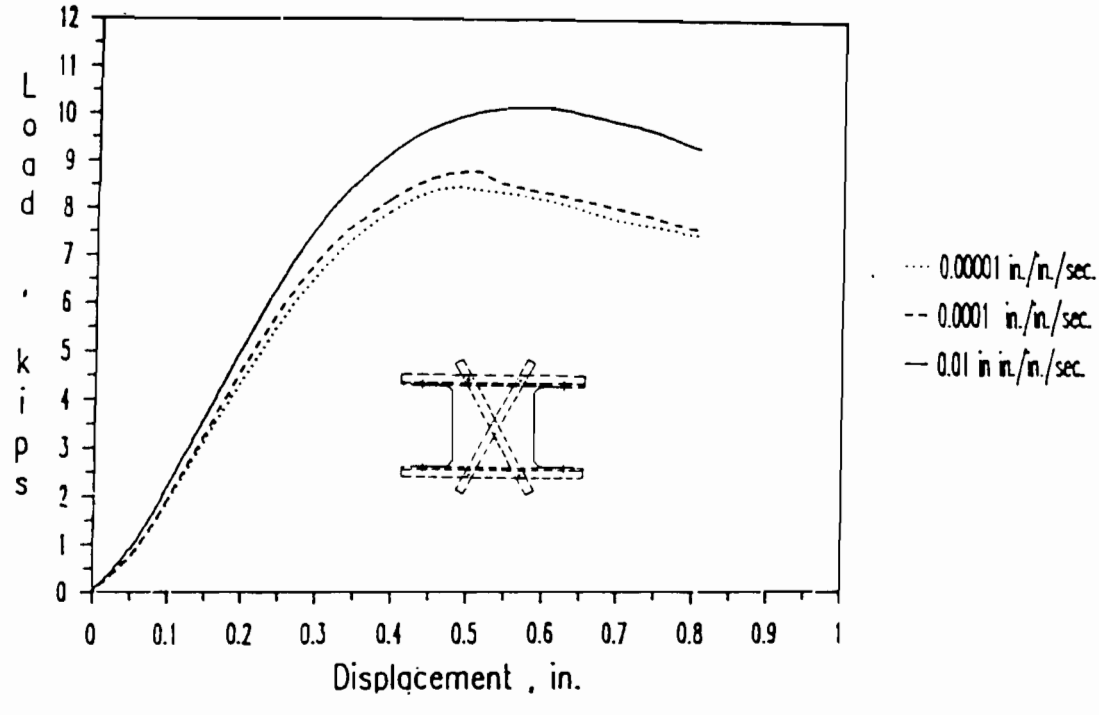

Figure 3.34 Load-Displacement Curves for Channel Beams Using 35XF Sheet Steel (for Unstiffened Compression Element, w/t = 20.95) (B18)

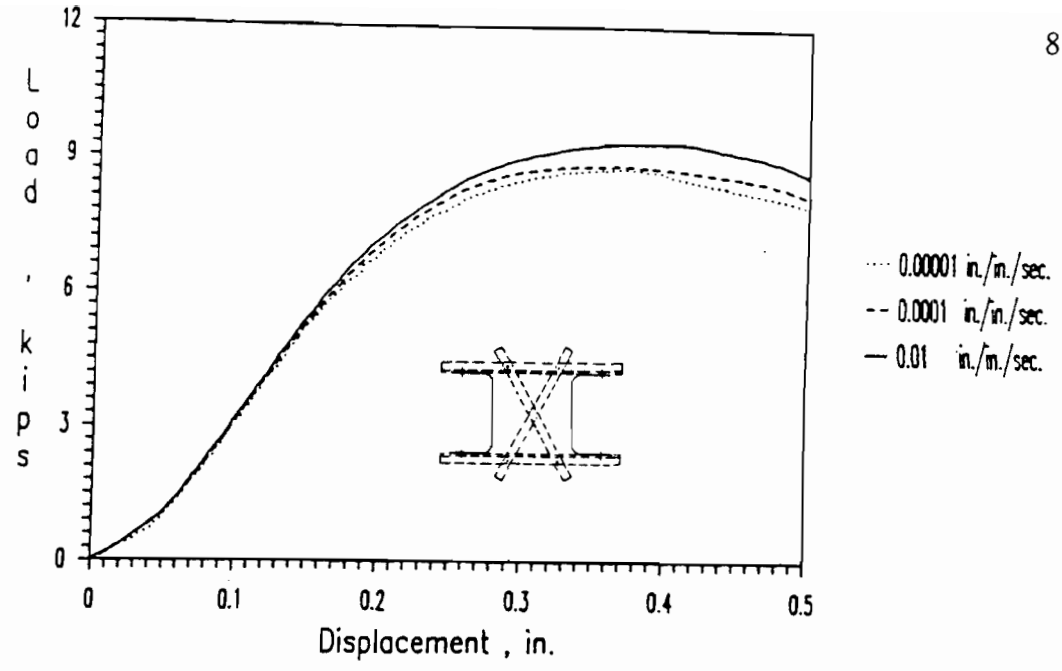

Figure 3.35 Load-Displacement Curves for Channel Beams Using 50XF Sheet Steel (for Unstiffened Compression Element, w/t = 8.83) (B18)

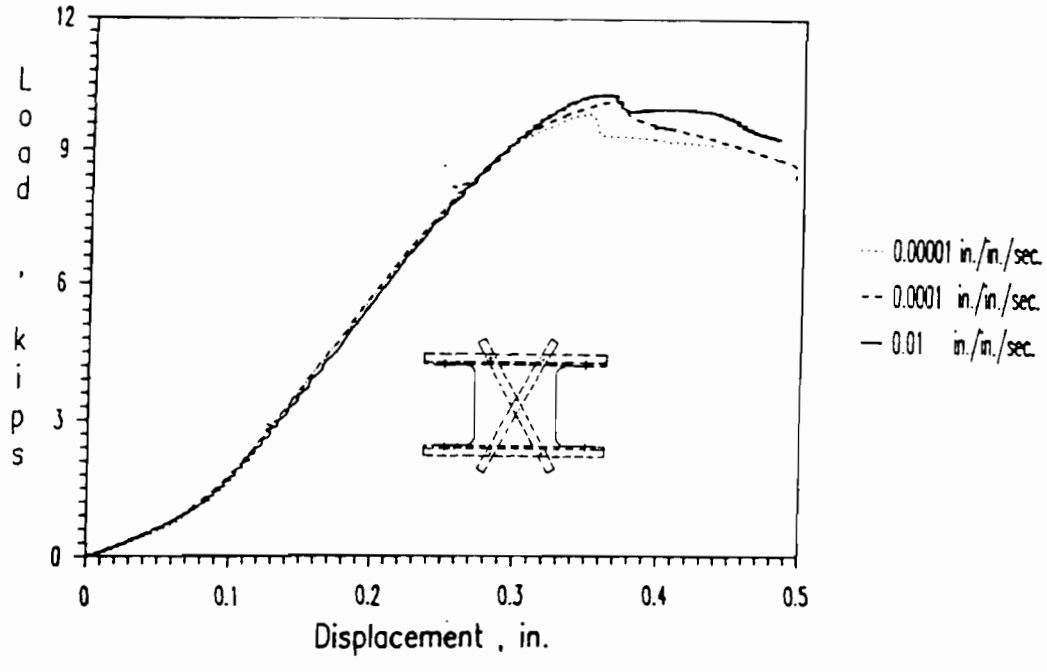

Figure 3.36 Load-Displacement Curves for Channel Beams Using 50XF Sheet Steel (for Unstiffened Compression Element, w/t = 15.33) (B18)

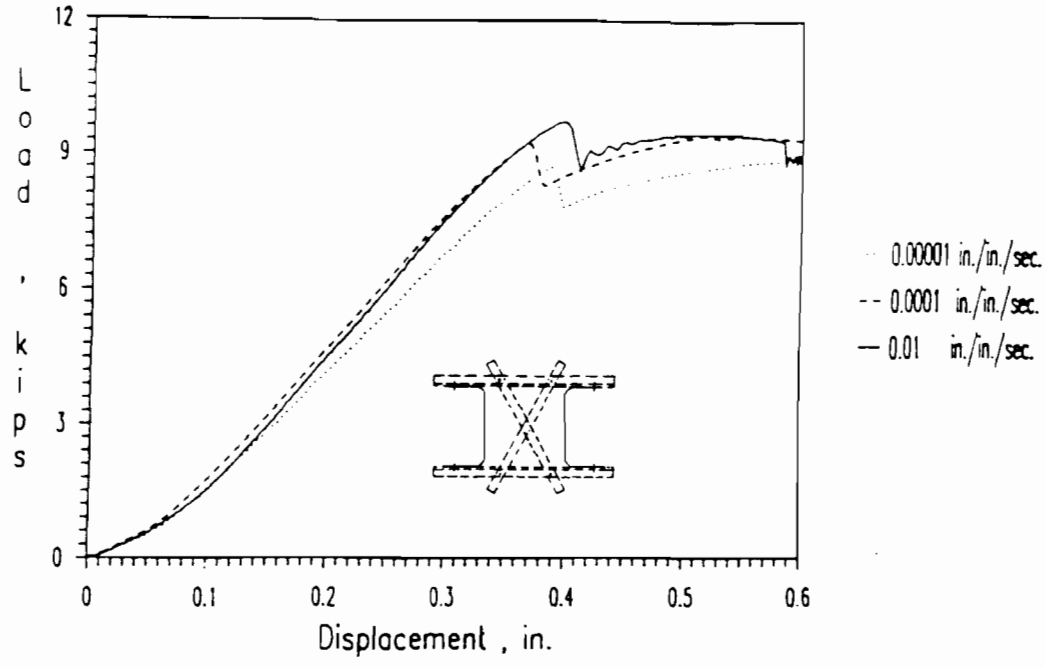

Figure 3.37 Load-Displacement Curves for Channel Beams Using 50XF Sheet Steel (for Unstiffened Compression Element, w/t = 20.51) (B18)

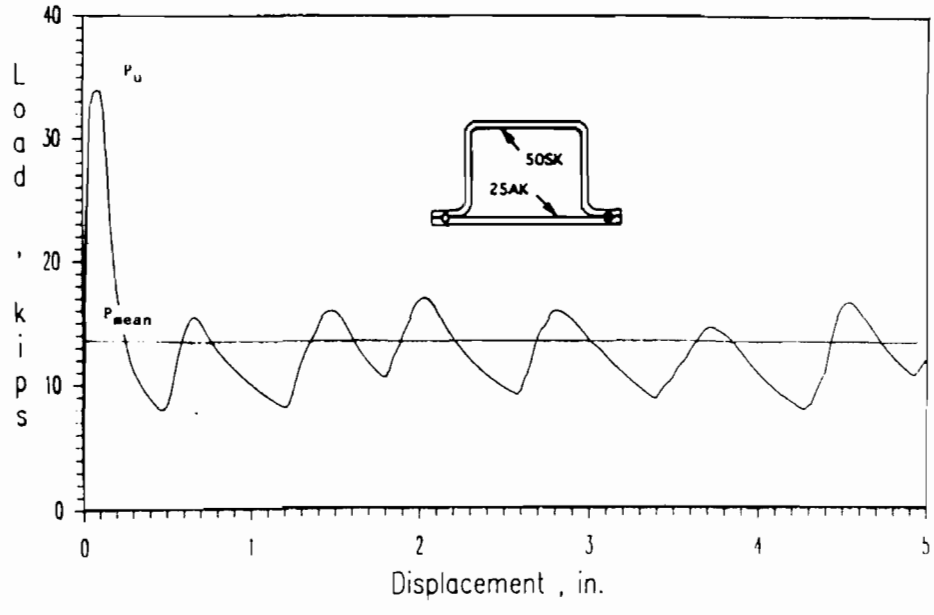

Figure 3.38 Typical Load-Displacement Curve of Hybrid Stub Columns (B19)

APPENDIX A

LOCAL BUCKLING COEFFICIENTS DERIVED BY KALYANARAMAN FOR UNSTIFFENED COMPRESSION ELEMENTS

According to Kalyanaraman, the following equations can be used to calculate the local buckling coefficient of unstiffened elements of I-shaped stub columns under axial compression:

$$K_e = 0.851 + 0.426\,(\varepsilon^{0.7} - 1.5)/(\varepsilon^{0.7} + 1.5) \qquad \text{(A1)}$$

$$K_p = 0.637 + 0.212\,(\varepsilon^{0.74} - 2.04)/(\varepsilon^{0.74} + 2.04) \qquad \text{(A2)}$$

In Equations A1 and A2, the subscripts *e* and *p* represent the elastic and plastic buckling coefficients, respectively. The symbol "ε" is a rotational edge restraint factor which can be determined by using the following equation:

$$\varepsilon = (B_b/B_r)\,(D_r/D_b)\,(C_f/N_b)S_r'' \qquad \text{(A3)}$$

In the above equation, B_b = width of bending element, B_r = width of restraining element, C_f = correction factor, D_b = flexural rigidity of the bending element, D_r = flexural rigidity of the restraining element, N_b = number of buckling elements at the junction, S_r'' = rotational edge stiffness.

The actual buckling coefficient, K, of a compression element can vary between K_e and K_p depending upon the yield stress (σ_y) and the element demensions. On the basis of the available test results, Kalyanaraman derived the following equations for determining the local buckling coefficient of unstiffened compression elements:

a. $K = K_e$ if $K_y \geq 1.25K_e$ (A4)

b. $K = K_e - (K_e - K_p)(1.25K_e - K_y) / (1.25K_e - K_y)$ if $1.25\ K_e \geq K_y \geq K_p$ (A5)

c. $K = K_p$ if $K_y \leq K_p$ (A6)

where $K_y = [\sigma_y 12(1-\mu^2)(B_b/t_b)^2] / \pi^2 E$ (A7)

σ_y = yield stress

t_b = thickness of element

E = modulus of elasticity